EARTHQUAKE SEGMENT BOUNDARIES AND TSUNAMIGENIC FAULTS OF THE KODIAK SEGMENT, ALASKA-ALEUTIAN SUBDUCTION ZONE

by

Marlon D. Ramos

A thesis

submitted in partial fulfillment

of the requirements for the degree of

Master of Science in Geophysics

Boise State University

August 2017

BOISE STATE UNIVERSITY GRADUATE COLLEGE

DEFENSE COMMITTEE AND FINAL READING APPROVALS

of the thesis submitted by

Marlon D. Ramos

Thesis Title: Earthquake Segment Boundaries and Tsunamigenic Faults of the Kodiak Segment, Alaska-Aleutian Subduction Zone

Date of Final Oral Examination: 25 April 2017

The following individuals read and discussed the thesis submitted by student Marlon D. Ramos, and they evaluated his presentation and response to questions during the final oral examination. They found that the student passed the final oral examination.

Lee M. Liberty, M.S.	Chair, Supervisory Committee
Dylan Mikesell, Ph.D.	Member, Supervisory Committee
Clyde J. Northrup, Ph.D.	Member, Supervisory Committee

The final reading approval of the thesis was granted by Lee M. Liberty, M.S. Chair of the Supervisory Committee. The thesis was approved by the Graduate College.

DEDICATION

I would like to dedicate this thesis to my childhood self. If there were such a thing as a time machine, I would use it to go back and show him all the potential he has. I would proffer this thesis, this body of scientific work, as evidence that with patience and steadfast commitment, he can do anything he sets his mind to. I would demonstrate that his future is brighter. Assure him that he can forge a new life – a better one.

ACKNOWLEDGEMENTS

First and foremost, I would like to acknowledge my thesis adviser, Lee Liberty. I deeply appreciate his teaching me how to ask the bigger questions, the ones that matter in this discipline. Under his tutelage, I was able to grow into a stronger scientist while at Boise State. He is an adept adviser and I respect him both as a member of the earthquake hazards community and as a person.

I extend my gratitude to the grad students of the ERB; especially those that call the third floor a second home. Stay golden.

I would be sorely remiss if I did not give credit to the dogs of the 3rd floor, as well. They are the true saviors, selflessly humoring us and enduring our incessant babbling about Helmholz decomposition, the Critical Zone, and dispersion curves (also for providing a shoulder to cry on when our flows in Promax refuse to run – which is, regrettably, admittedly, tragically… often).

ABSTRACT

The most recent megathrust earthquake to impact the Alaska subduction zone was the M9.2 Great Alaska earthquake of 1964. This multi-segment rupture spanned over 700 km of the plate boundary and engendered both local and trans-Pacific tsunamis. The Kodiak Islands region served as the southwestern limit to rupture. The nature of past megathrust segmentation for the Alaska subduction zone has been largely hypothesized through paleoseismological methods and the Kodiak region in particular has not received a comprehensive geophysical characterization of its inferred segment boundaries.

I analyze multiple geophysical datasets (e.g. seismic reflection, earthquake, potential fields) to understand the spatiotemporal relationships between subduction, accretion, lower and upper plate structure, and tsunamigenic fault hazard in the context of the known megathrust earthquake record and other interseismic observations for the Kodiak region.

The northeast Kodiak segment boundary is defined by the subducting 58° fracture zone, which can be traced below the forearc using magnetic and gravitational fields. Subduction of this feature is expressed on post-1964 seismicity, is consistent with oblique shortening, and manifests itself within the upper plate as the Portlock Anticline.

The southwest segment boundary marks the transition between the Kodiak and Semidi segments. It is shown to be a region that shifts from significant margin erosion to a region of imbricate thrusting and margin growth. These two zones are bound by fracture zone subduction. I furthermore independently constrain and compliment

paleoseismological models of joint Kodiak and Semidi segment rupture by identifying and characterizing a through-going marine fault zone across this segment boundary.

Finally, I revisit the source mechanisms for the local tsunami that inundated the Kodiak Islands as a result of the 1964 earthquake. I provide a new tsunamigenic source model that suggests discrete uplift of the Kodiak Islands shelf fault system and illuminate its along-strike rupture variability throughout the Holoecene epoch.

My findings suggest segment boundaries across Kodiak have a clear geophysical expression and a multi-dataset approach is necessary to decipher tectonic controls on megathrust segmentation.

TABLE OF CONTENTS

LIST OF TABLES

LIST OF FIGURES

LIST OF ABBREVIATIONS

ABfz	Albatross Banks fault zone
ALEUT	Alaska Langseth Experiment to Understand the megaThrust
AFz	Aja Fracture Zone
ANSS	Advanced National Seismic System
CDP	Common Depth Point
CMT	Centroid Moment Tensor
DEM	Digital Elevation Model
EMAG2	Earth Magnetic Anomaly Grid (2 arc-min resolution)
FIR	Finite Impulse Response
GPS	Global Positioning System
GFA	Free Air Gravity Anomaly
GFA_{pw}	Pseudo-Bouguer Free Air Gravity Anomaly
g_{UP}	Upward-continued gravity field
h	height relative to a given datum (measured in meters)
K	Wavenumber matrix in either x or y spatial dimension
KB	Kodiak-Bowie
kg	Kilogram
km	Kilometer
ka	“kiloannum” (thousand years ago)
KSfz	Kodiak Shelf fault zone

LGM	Last Glacial Maxima
m	Meters
m/s	meters per second
Ma	“megaannum” (million years ago)
mGal	miligal (1 Gal = 1 cm per second squared), a unit of gravity
MMS	Mineral Management Services of Alaska
Mw	Moment-magnitude (a measure of earthquake energy
mm/yr	millimeters per year
NOAA	National Oceanic and Atmospheric Administration
NOS	National Ocean Service
PM	Patton-Murray
PWS	Prince William Sound
s	seconds
TACT	Trans-Alaska Crustal Transect
USGS	United States Geological Survey

CHAPTER ONE: INTRODUCTION

Subduction zones host the world's largest earthquakes (M>8) and are the source of strong ground motion and tsunamis that can have disastrous effects on coastal populations globally. The generalized anatomical profile of a subduction zone is portrayed in Figure 1a. Considerations of incoming plate sediment flux and lithology, convergence rate, plate age, and whether the forearc (region between magmatic front and trench) is in an accretionary or erosional stage all influence seismogenesis (Stern, 2002). Despite the large scale of a subduction system (~100's of km), it is typically only the shallowest region between the overriding and subducting plate that can generate large earthquakes. These large earthquakes are the result of stress release along asperities (stuck patches) of the plate boundary, or megathrust that separates mostly dense oceanic crust subducting beneath less dense continental material (Lay et al., 1982; Figure 1b).

The Alaska subduction zone accommodates a 50 - 70 mm/yr northward migration of the Pacific plate beneath the North American plate (DeMets et al., 2010). Over the past century, nearly all segments of this plate boundary have coseismically ruptured, and many have produced damaging tsunamigenic earthquakes (Carver and Plafker, 2008; Ryan et al., 2011). The eastern region of this subduction zone, beneath Prince William Sound (PWS) and the Gulf of Alaska, sourced the Earth's second-largest instrumentally recorded earthquake: the M9.2 Great Alaska Earthquake of 1964 (Plafker, 1969).

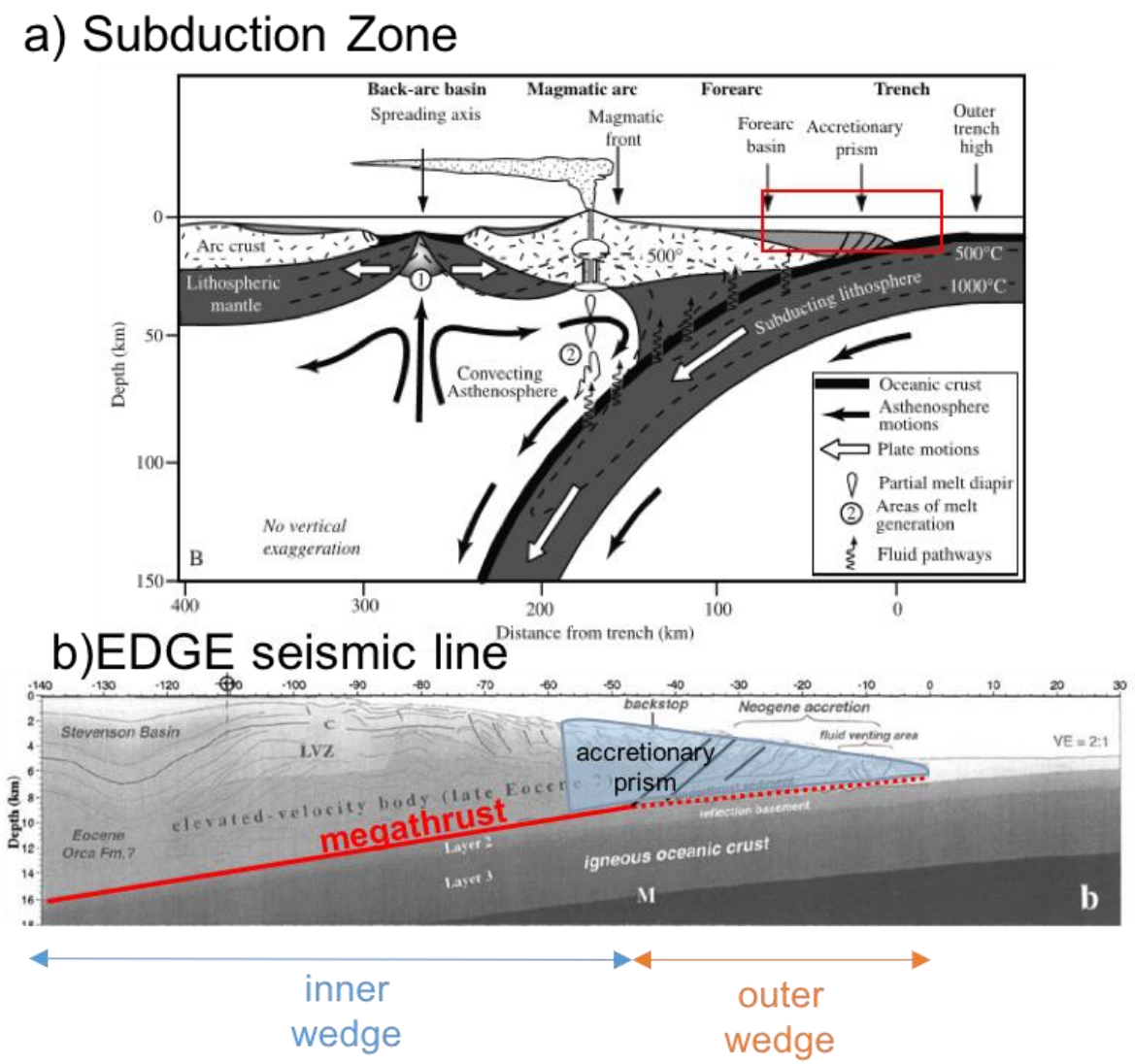

Figure 1. a) Generalized cross-section of a subduction zone. The seismogenic region is typically confined to the upper 50 km and the bulk of elastic deformation takes place within the arc-trench complex (modified from Stern, 2002). Inset red box shows a close-up of the forearc-trench complex close-up. b) Interpreted seismic refraction line (EDGE) from Gulf of Alaska shelf detailing accretionary prism structure (modified from Ye et al., 1997.) Bold red line along interface denotes the megathrust (or primary detachment between the upper and lower plates) with faults splaying from this boundary (black lines). The outermost forearc is further subdivided into the brittle outer wedge and more ductile inner wedge (Wang and Hu, 2006). Splay faults related to local tsunamigenesis cut forearc structures within the inner wedge.

The M9.2 1964 earthquake nucleated at a depth of about 20 km beneath PWS (Brocher et al., 1994). The earthquake produced strong ground shaking as far away as Anchorage and generated both local and transoceanic tsunamis (Plafker, 1969). A total rupture length of more than 700 km along the Gulf of Alaska was partitioned across three separate regions of the megathrust plate boundary, hereafter referred to as the PWS, Kenai, and Kodiak segments (Ichinose et al., 2007; Kelsey et al., 2015), but did not rupture the Semidi segment that is located to the west of the Kodiak Islands. Segment boundaries exist due to a heterogeneous plate interface that is related to complexities in plate coupling and interplate geometry (Ruff and Kanimori, 1983; Scholz and Campos, 2012). Although the 1964 earthquake ruptured three presumed segments, it is unclear what role these boundaries may play through many earthquake cycles.

The Yakutat terrane overlies the Pacific plate below PWS, and the eastern and western limits of the Yakutat terrane define the PWS segment boundaries (Figure 2). Subduction of the relatively buoyant Yakutat terrane has resulted in high seismic coupling for much of the PWS segment (Brocher et al., 1994; Zweck et al., 2002). A recurrence interval on the order of 700-800 years has been calculated for ~M9 (multi-segment) ruptures related to the PWS region (Huchinson et al., 2007; Shennan et al., 2009). In contrast, paleoseismic studies around the Kodiak region estimate recurrence intervals of 500-600 years for ~M8 earthquakes; and previous investigations suggest subducting morphologies on the incoming Pacific plate spatially define the rupture limits of many Kodiak initiated earthquakes (von Huene et al., 1999; Carver and Plafker, 2008).

Elastic strain on the upper plate is relieved during a megathrust earthquake such that landward regions of the upper plate typically experience coseismic subsidence while regions

within the outer forearc and accretionary prism typically uplift in response to slip (Plafker, 1972; Dragert et al., 1994). The region of differential uplift is where tsunamis can be set into motion. A trans-Pacific tsunami resulting from slip on faults that splay from the megathrust were responsible for deaths across the eastern Pacific Ocean in 1964; however, local tsunamis arriving on mainland Alaska and key islands were also engendered from both tectonic and landslide sources (Plafker, 1969; Ryan et al., 2011; Haeussler et al., 2015; Brothers et al., 2016).

Figure 2 delimits the Gulf of Alaska segments that have been proposed based largely from paleoseismic studies (Carver and Plafker, 2008; Briggs et al., 2014; Shennan et al., 2014; Kelsey et al., 2015). Table 1 lists the age ranges for each documented megathrust rupture in the vicinity of the Kodiak Islands. From an earthquake hazard perspective, it is important to constrain the recurrence interval of characteristic or damaging ruptures, identify segment boundary limits, and characterize faults that splay from the megathrust that could contribute to tsunamigenesis.

Many studies have identified and characterized the PWS segment properties through various geophysical and geological investigations (Brocher et al., 1994; Eberhart-Phillips et al., 2006; Liberty et al., 2013; Kim et al., 2014). Similar literature exists for the Semidi segment that spans the region to the southwest of the Kodiak Islands (Johnson and Satake, 1994; Fournier and Freymueller, 2007; Shillington et al., 2015). However, segment boundaries for the Kodiak region have been largely defined by island-based paleoseismic studies and the inferred behavior of subducted lower plate topography from seismicity (von Huene et al., 1999; Doser et al., 2002; von Huene et al., 2012; Briggs et al., 2014; Shennan et al., 2014).

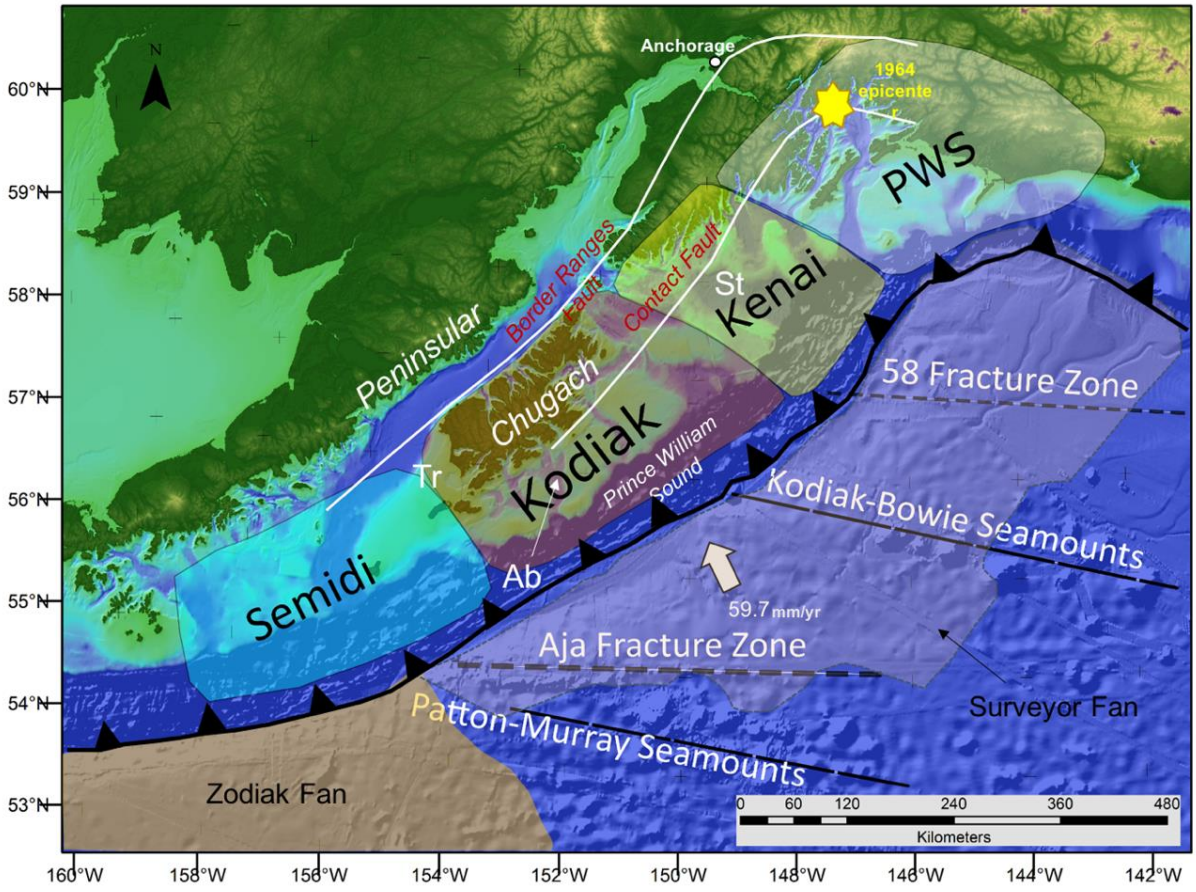

Figure 2. a) Tectonic map of the Gulf of Alaska region showing subduction zone segments and major topographic and structural features on the North American and Pacific plates. These plates are separated by the Aleutian trench (black hachure lines). The 1964 Great Alaska earthquake epicenter is labeled. Shaded regions on the North American plate denote different segments as inferred from paleoseismological studies (see Table 1). The major structural boundaries are labeled in white (Peninsular, Chugach, and Prince William Sound terranes); the Border Ranges and Contact faults (red) denote terrane boundaries. Ab, Tr, and St stand for the Albatross, Trinity, and Stevenson Basins, respectively. Convergence rate from MORVEL plate velocity model (DeMets et al., 2010). The two major deep-sea fans (Surveyor and Zodiak) are depicted as shaded regions on the incoming Pacific plate (Stevenson and Embley, 1987; Gulick et al., 2015).

In this thesis, I explore the geophysical expression of the presumed Kodiak segment boundaries by analyzing several geophysical datasets (potential fields, seismic reflection, and seismicity data) in the context of lower and upper plate structure. I then relate these boundaries to the megathrust earthquake record and to conditions beneath the forearc region

along the megathrust boundary. I also independently constrain the tsunami source location that 1) impacted the Kodiak Islands as a result of the 1964 earthquake and; 2) may impact the region during future large earthquakes by identifying locations of past vertical uplift accommodated along marine fault zones.

My thesis highlights the physical expression of segment boundaries, enhances our knowledge of tsunamigenic fault hazard, and reconciles multiple datasets to give a holistic tectonic picture of the Kodiak segment in the Alaska-Aleutian subduction zone. Chapter 2 provides the geophysical data, methodology, and constraints I then draw upon in my analysis and interpretation of these data. Chapter 3 discusses the geophysical signature and tectonic influence of the subducting 58° fracture zone. In Chapter 4, I provide new spatial constraints on the local tsunami from 1964 and characterize the Kodiak Shelf fault zone that my models suggest sourced this tsunami. Chapter 5 shows the interseismic and geologic expression of the southwest segment boundary with key constraints on lower crustal structure provided by earthquake and magnetic data; I also identify the continuation of the near-shore marine fault zone discussed in Chapter 4.

Geologic and Seismotectonic Setting: Kodiak Islands region, Alaska

Tectonics

The Kodiak Islands are a mid-forearc high consisting of Late-Cretaceous to Neogene accretionary complexes that were built and uplifted in response to subduction over the last 100 Ma (Moore et al., 1983; Plafker et al., 1994; Carver and Plafker, 2008). At least four different oceanic plates have subducted to shape present day Alaska and the Kodiak region: the Resurrection, Farallon, Kula, and Pacific plates (Plafker et al., 1994; Haeussler et al., 2003). Major seafloor structures on the incoming Pacific plate offshore of the Kodiak

Islands include the Kodiak-Bowie (KB) and Patton-Murray (PM) seamount chains and the Aja (AFz) and 58° fracture zones (Naugler and Wageman, 1973; von Huene et al., 1999; von Huene et al., 2012; Figure 2). In contrast to the PWS segment, the Kenai and Kodiak segments involve the subduction of only Pacific plate rocks and contains less sediment above incoming plate mafic rocks. Higher density and greater westward age of the subducting oceanic lithosphere result in a steepening of the subduction angle (Plafker et al., 1994; von Huene et al., 1980; Eberhart-Phillips et al., 2006; Kim et al., 2014). The presumed subduction angle for the Kodiak Islands region is about 8 degrees and steepens to the north beneath mainland Alaska (Hayes et al., 2012).

Large scale structure from potential fields

The gravity signature over subduction zones reflect incoming and upper plate structure and can give a perspective on seismogenic properties. Wells et al. (2003) explored the correlation between negative free-air gravity anomalies, forearc basins, and asperity location for several great megathrust earthquakes. Similarly, Song and Simons (2003) related trench-parallel variations in the gravity field to frictional conditions at the interface, which favor unstable sliding (i.e. stick-slick behavior) over Ma time scales. However, recent studies have pointed out that such simple correlations between low density basin depocenters and maximum moment-release do not correlate to slip patterns observed after the Great Alaska Earthquake of 1964, or other more recent earthquakes (Ichinose et al., 2007; Ammon et al., 2011). For the Kodiak forearc region, a strong positive free-air gravity signature has been speculated to result from exceptionally thick or anomalously dense oceanic material and has been noted by multiple authors (Wells et al., 2003; Song and Simons, 2003). Basset and Watts (2015a, b) pioneered a new technique to isolate and

remove the average free-air gravity or topography signal in the frequency domain (i.e. subtracting the average wavelength spectral component from the gravity field) to uncover short wavelength structure; this approach can highlight subducted seamounts, seafloor ridges, or splay faults within the shallow forearc region (Basset and Watts 2015a; Basset and Watts, 2015b).

Kodiak Islands forearc and terrane boundaries

Two major trench-parallel structural boundaries have been mapped across the Gulf of Alaska, and these boundaries separate tectonic provinces around the Kodiak Islands. The Border Ranges fault zone separates the Paleogene Chugach and Peninsula terranes landward of the Kodiak Islands and along the Kenai Peninsula (Figure 2). This boundary has a clear gravity expression (Figure 3) and served to limit northward rupture during the 1964 earthquake. The Contact fault zone is mapped to the seaward side of Kodiak Island and north of PWS. This fault corresponds to the transition between uplift and subsidence during the 1964 earthquake.

The Kodiak Islands segment has undergone several episodes of accretion that were driven mostly by climate cycles (Fisher and von Huene, 1980; Moore and Allwardt, 1980; Clendenen et al., 1990). Forearc strata within the Kodiak segment is comprised of Cenozoic Chugach and Prince William terranes that decrease in age to the south and are separated by the Contact fault (Plafker et al., 1994). The broad and well-developed forearc of the Prince William terrane includes several prominent sedimentary basins in the present day inner prism (Tugidak, Albatross, and Stevenson basins) whose growth were coeval with interseismic uplift and accretion (Fisher and Bryne, 1987; Moore et al., 1991). Clendenen et al. (1990) estimated as much as four kilometers of Neogene uplift across the Albatross basin

region with sediment subduction, underplating, and underthrusting all contributing to forearc physiography.

Most sediment contributions to the Kodiak trench stem from the Surveyor deep marine fan with a minor component from the Zodiac fan (Figure 2). The Surveyor fan has subsisted for the last 20 Mya and attains a local thickness of ~4 km offshore present-day PWS. Sediment supply diminishes to the southwest until its southern terminus at the PM Seamount chain (Reece et al., 2011). On the other hand, the Zodiac fan is sourced from Cook Inlet sediments and is the primary sediment source for the adjacent Semidi segment (Stevenson and Embley, 1987; von Huene et al., 2012). The general trend of both marine fans is one of decreasing sediment thickness towards the southwest along the North America and Pacific plate margin (Reece et al., 2011). Sediment thickness in the vicinity of the Kodiak segment can be on the order of ~ 2 km. (Gulick et al., 2015).

Crustal Structure

A myriad of bathymetric and active-source seismic data provide constraints on upper plate structure and seafloor topography. Crustal-scale seismic reflection and refraction experiments such as EDGE, TACT, and ALEUT have imaged the megathrust boundary, sediment channel underplating, and splay faults (Moore et al., 1991; Brocher et al., 1994; Ye et al., 1997; Fruehn et al., 1999; Li et al., 2013; Liberty et al., 2013; Haeussler et al., 2015). The EDGE seismic experiment imaged a 2.5 degree dipping megathrust below a Neogene accretionary prism (see Figure 1b) and a crustal velocity model was constructed from ocean bottom seismometer data showing anomalously low velocities beneath the Kenai/Kodiak segment boundary (Moore et al., 1991; Ye et al., 1997). Ye et al. (1997) attributed this low velocity zone to a subducted seamount.

Submarine fault systems

There are numerous presumed splay faults that cross the Kodiak forearc that is located seaward of the Kodiak Islands. Previous studies have identified two primary fault systems, the Kodiak Island shelf (KSfz) and Albatross Banks (ABfz) fault zones, which are contiguous in the region immediately offshore of the Kodiak Islands to the continental shelf (von Huene et al., 1980; Carver et al., 2008). Limited seismic imaging results suggest faults associated with the ABfz are a series of imbricate thrusts that are a part of a larger fold and thrust system extending almost to the continental shelf break (von Huene et al., 1980). Faults associated with the ABfz are near vertical and tend to control the formation of anticlines that bound forearc basins.

The KSfz includes the Narrow Cape and Kodiak Islands fault zones, where both have an onshore component on the Kodiak Islands. From onshore data, Carver et al. (2008) documented the Narrow Cape paleoseismic history that suggests a recurrence interval of 1-2 ka for surface rupture events, more than four times the average recurrence interval (at maximum) for the entire Kodiak segment. Vintage seismic imaging of the KSfz reveal high-angle faults where bedrock exposures in the hanging wall suggest that uplift has exceeded deposition for the past few earthquake cycles (Fisher and von Huene, 1980; von Huene et al., 1980).

Tsunami inversions of teleseismic tide gauge records from 1964 estimate peak slip, which generated a trans-Pacific tsunami, to originate from the continental slope region (Johnson and Satake, 1994; Ichinose et al., 2007). While these models preferentially assign maximum slip to occur along the continental slope region (Suleimani et al., 2003), local tsunamis are often sourced from faults along the continental shelf. Splay fault slip through

the imbricate outer wedge is appropriate for trans-Pacific tsunamigenesis, but does not agree with the short (< 60 min) travel times tabulated in the Plafker (1969) report. The 1964 event inundated several locations on mainland Kodiak Island and the local tsunami source region was inferred to be one of several linear fault sources to the south or east of the Kodiak Islands (Plafker, 1969). I will provide important constraints on this local tsunami source in Chapter 4.

Geodesy

In the context of subduction zones, interplate or seismic coupling is the ability of the megathrust to lock and accumulate stress (Ruff and Kanimori, 1983). High coupling means that the fault is locked and capable of producing large coseismic release in the form of earthquakes. Geodetic GPS models incorporating viscoelastic and non-viscoelastic behavior show that the Kodiak segment is highly locked near the southwest boundary with the Semidi segment while the degree of locking along the central and eastern portions of the segment are considerably less (Zweck et al., 2002; Suito and Freymueller, 2009). Horizontal GPS velocities onshore Kodiak suggest an upper mantle viscoelastic response, after-slip from 1964, and creep are all present in the geodetic signal (Sauber et al., 2006). Doser et al. (2002) noted higher post-1964 lower plate moment-release in the southwest region of Kodiak segment relative to other portions of this segment and with adjacent segments. A possible reason for this higher moment release may be related to stress-loading of the shallow seismogenic zone due to downdip creep on the locked megathrust (Sauber et al., 2006). However, there is room for interpretation in this result as several large post-1964 earthquakes (M > 5) have occurred immediately below the outer wedge.

Kodiak segment seismicity

The Kodiak segment has experienced larger and more frequent interseismic events relative to the PWS and Kenai segments both before and after the 1964 event (Doser et al., 2002; Doser, 2005; Doser, 2006). Large modern earthquakes have mostly occurred in the southwest Kodiak region, with a majority of these events presumably nucleating within the subducting Pacific slab (Ratchkovski and Hansen, 2001; Doser et al., 2002). In contrast, there has been a paucity of pre and post-1964 large earthquakes associated with the eastern and central portions of the Kodiak segment (Doser et al., 2002). These observations suggest that consistent seismotectonic controls have persisted along the Kodiak segment for multiple megathrust earthquake cycles, and a kinematic, structural model for these observations has yet to be invoked. Chapter 5 of my thesis explores this relationship.

Table 1.1 Spatiotemporal megathrust rupture history for the Kodiak region.

Segment(s)	Time of Rupture	Single or Multi-segment	Source
Kodiak/Kenai/PWS	AD 1964	Multiple (3)	Ichinose et al. (2007)
Semidi	AD 1938	Single	Johnson and Satake (1994)
Kodiak/Semidi	AD 1788	Multiple (2)	Briggs et al. (2014)
Kenai	AD 1530 - 1840	Single	Shennan et al. (2014)
Kodiak or Kodiak/Kenai	AD 1430 - 1650	Single or Multiple (2)	Briggs et al. (2014) Kelsey et al. (2015)
Kodiak/Kenai/PWS	AD 1060 - 1110	Multiple (3)	Kelsey et al. (2015)

CHAPTER TWO: DATA AND METHODOLOGY

Free-Air Marine Gravity

I utilize a global free-air gravity dataset available through the Scripps Institute of Oceanography (http://topex.ucsd.edu/cgi-bin/get_data.cgi, last accessed on 2016/03/05). The vertical component of the gravity field is computed via satellite altimetry measurements and details of its derivation can be found in Smith and Sandwell (1997).

I apply several field transformation algorithms and filtering techniques to the free-air anomaly in order to extract long and short wavelength features from the global gravity field. My goal is to highlight upper and lower crustal density variations across the forearc and relate lineations to subducted morphology of the incoming plate and upper plate splay faults.

Pseudo-Bouguer correction

The free-air correction to gravity measurements accounts for differences in elevation between the geoid and the location where the measurement is made (Blakely, 1996). Free-air gravity anomalies can closely mimic continental or oceanic lithosphere topography due to elevation dependence on the free-air correction (Lowrie, 2007).

The density effect of seawater is strongest above the ocean trench, where the water depth is greatest (~220 mGals offshore Kodiak Island). To account for this effect, I calculate the Bouguer anomaly of seawater for all elevations below sea-level assuming a uniform density for seawater (1030 kg/m^3) and subtract these values from the original free-air anomaly as follows

$$\Delta g_b = 2\pi\gamma\rho \quad (1)$$

$$GFA_{pw} = g_{FA} - \Delta g_b h \quad (2)$$

where Δg_b is the Bouguer anomaly, γ is the universal gravitational constant (6.674 x 10^{-11} $m^3kg^{-1}s^2$), h is the water depth in meters, and g_{FA} is the free-air anomaly (e.g., Blakely, 1996). Essentially, this removes the gravity contribution of seawater density from the free-air anomaly. I will refer to this re-expression of the free-air anomaly as the pseudo-Bouguer free-air anomaly, or GFA_{pw}. Note that the GFA_{pw} does not assume densities of the continental or oceanic lithosphere so it is not a true Bouguer correction. A side by side comparison of the free-air and GFA_{pw} anomalies is shown in Figure 3.

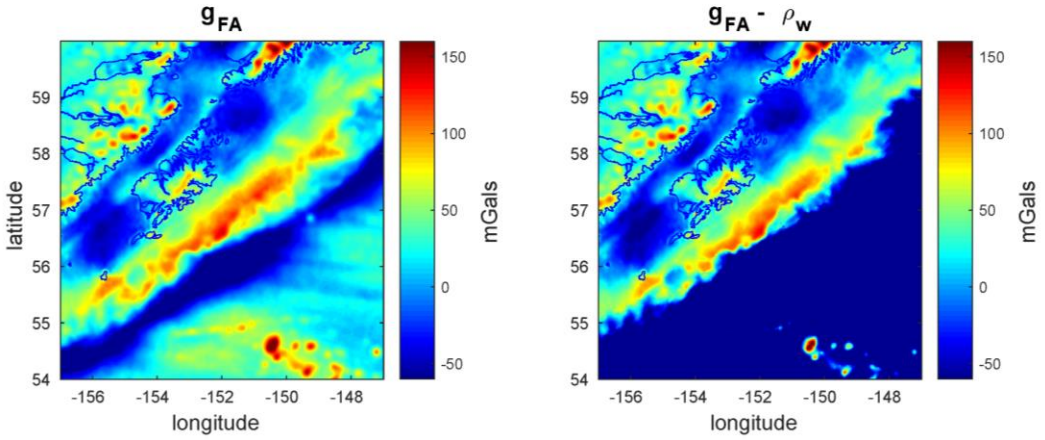

Figure 3. Left: marine free-air gravity anomaly map. Right: marine free air gravity anomaly map with Bouguer correction for seawater density. Dark blue line delimits the Kodiak Islands and Alaska Peninsula coastline.

Upward continuation of the gravity field

Upward continuation is a linear filter that attenuates short-wavelength signals in the gravity field by mapping the original field to a new datum located at a greater height above the surface (e.g., Blakely, 1996). This transformation is accomplished by

calculating the two-dimensional Fourier transform of GFA_{pw} and then multiplying by a wavenumber filter kernel in the frequency domain. Then, the inverse Fourier transform is applied to their product to yield the upward-continued gravity field (Equations 3 – 5)

$$G_k = \Im[GFA_{pw}] \quad 3$$

$$\Phi = e^{-zK}, \text{ filter kernel} \quad 4$$

$$g_{UP} = \Im^{-1}[G_k \cdot \Phi] \quad 5$$

where z is a positive quantity that indicates the upward-continuation height in meters, k_x and k_y are cycles per wavelength in the x and y directions, respectively, K is the wave number matrix equal to $\sqrt{k_x^2 + k_y^2}$, Φ is the filter kernel in the spatial frequency domain (i.e. wavenumber), g_{UP} is the upward continued signal, and $\Im$ and $\Im^{-1}$ denote the forward and inverse Fourier transforms, respectively. Figure 4 depicts the GFA_{pw} upward continued to a height of z = 3 km above the original measurement datum.

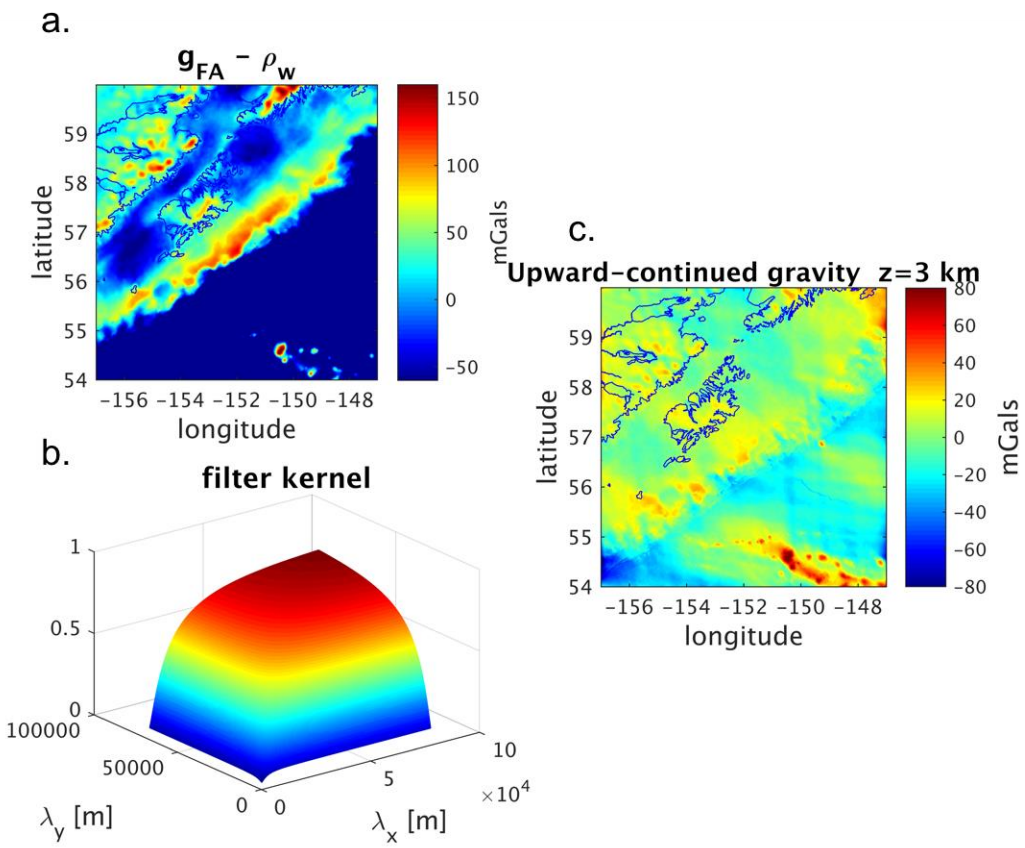

Figure 4. a) GFApw. b) filter kernel Φ to be multiplied by the 2-D Fourier transform of a. c) filtered result upward continued to height z = 3 km. Note gravity lineations on the Pacific plate seafloor corresponding to seamount chains and fracture zones. The forearc region offshore of the Kodiak Islands also retains some positive gravity highs.

Wavelength filtering

I also apply a series of low and high pass wavelength finite impulse response filters (FIR) to accentuate different structures in the gravity data. Filtered data were subtracted from the original gravity signal to obtain maps containing complementary long or short wavelength components (Figure 5).

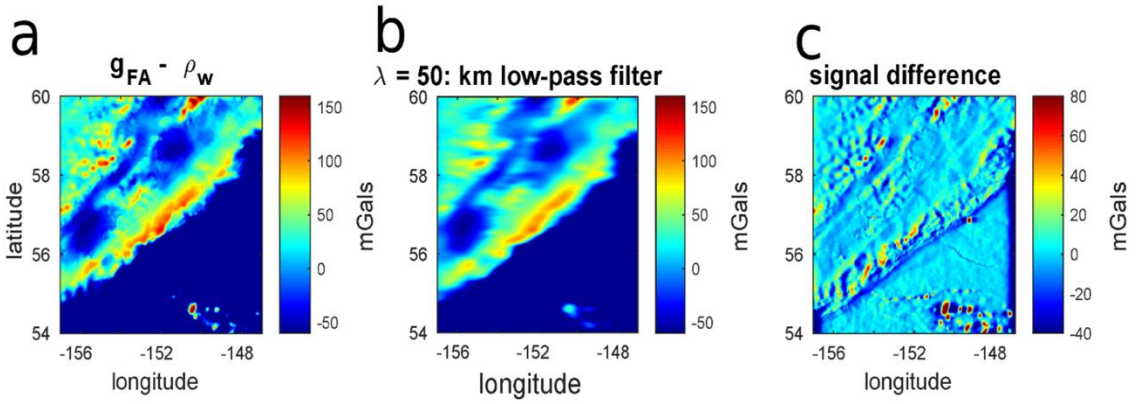

Figure 5. a) GFApw. b) low-pass filtered gravity field. c) subtraction of b from a (i.e. short-wavelength component of the gravity field).

Seafloor Topography and Bathymetry data

Dense repeat surveys of satellite altimeter measurements are used to construct maps of the seafloor (Smith and Sandwell, 1997; Sandwell et al., 2014). There exists a complementary dataset to the free-air gravity dataset which I used in my calculation of the pseudo-Bouguer gravity anomaly (http://topex.ucsd.edu/cgi-bin/get_data.cgi, 2016/03/05).

For the tsunami modeling aspect of my thesis, I relied on high-resolution (relative to satellite based topography) bathymetry data points available from NOS Bathymetric surveys through NOAA (https://maps.ngdc.noaa.gov/viewers/bathymetry/, last accessed on 2015/11/01). Certain maps in Chapters 3 and 4 of this thesis are created using a DEM (Digital Elevation Model) from the Southern Gulf of Alaska Coastal Relief Model, as well (https://www.ngdc.noaa.gov/mgg/coastal/s_alaska.html; Lim et al., 2011).

Magnetics

The total-magnetic field anomaly is an important constraint to estimate magnetic susceptibility of the incoming plate. The EMAG2 (Earth Magnetic Anomaly Grid 2 Arc-minute resolution) is a compilation of magnetic field measurements compiled from

satellite, ship, and airborne datasets (Maus, 2009). I use the EMAG2 dataset as a constraint for my tectonic interpretations and as a comparison against other geophysical datasets (e.g. gravity, seismicity, seismic reflection). For example, the southern edge of the Yakutat plate is clearly seen on the total-magnetic field map (Figure 6).

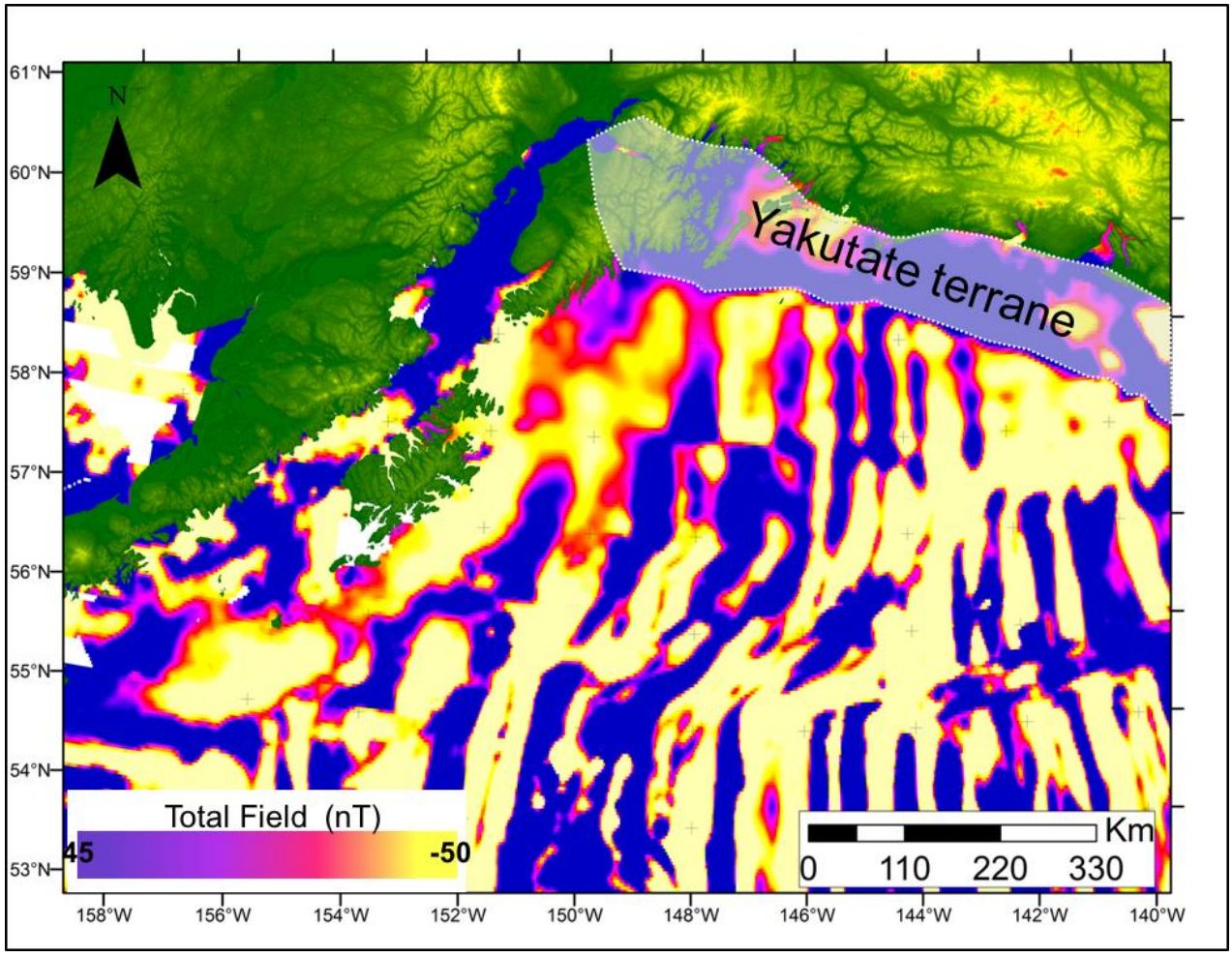

Figure 6. Total-field magnetic anomaly of the Gulf of the Alaska (Maus, 2009). The trailing edge of the Yakutat terrane and western limit of the PWS segment is outlined.

Earthquake and Focal Mechanisms databases

Following the 1964 Great Alaska Earthquake, there have been over 50 earthquakes of moment-magnitude (Mw) greater than 5 across the Kodiak segment. I utilize the ANSS earthquake and Harvard Centroid Moment Tensor (CMT) (Dziewonski

et al., 1981; Ekstrom et al., 2012) catalogs to estimate seismic moment release and seismic flux for events in the southwest and northeast regions of Kodiak. The seismic flux is (Scholz and Campos, 2012)

$$P_s = \frac{M_o}{\mu} = \int u \, dA \qquad 6$$

where Mo is the seismic moment, μ is the shear modulus, u is the displacement, and dA is the area where seismic energy is being released from. The time derivative of seismic flux is the seismic flux release-rate. The seismic coupling coefficient (X_s) is the ratio of seismic-flux release rate to the convergence rate of the incoming plate:

$$X_s = \frac{dP_S}{dP_T} \qquad 7$$

where dP_s is the moment-release rate (time derivative of equation 6) and dP_T is the tectonic flux rate, or simply the plate convergence rate multiplied by the average area of plate coupling along the subduction zone interface. Seismic flux is thus a fundamental parameter to quantitative seismotectonics and is indirectly related to seismic coupling.

From the spatiotemporal pattern of large magnitude and well-located events (CMT solutions), I will present a tectonic interpretation of interseismic (post-1964) deformation in Chapter 4. Figure 7 shows the earthquake catalog in the context of the 1964 aftershock zone.

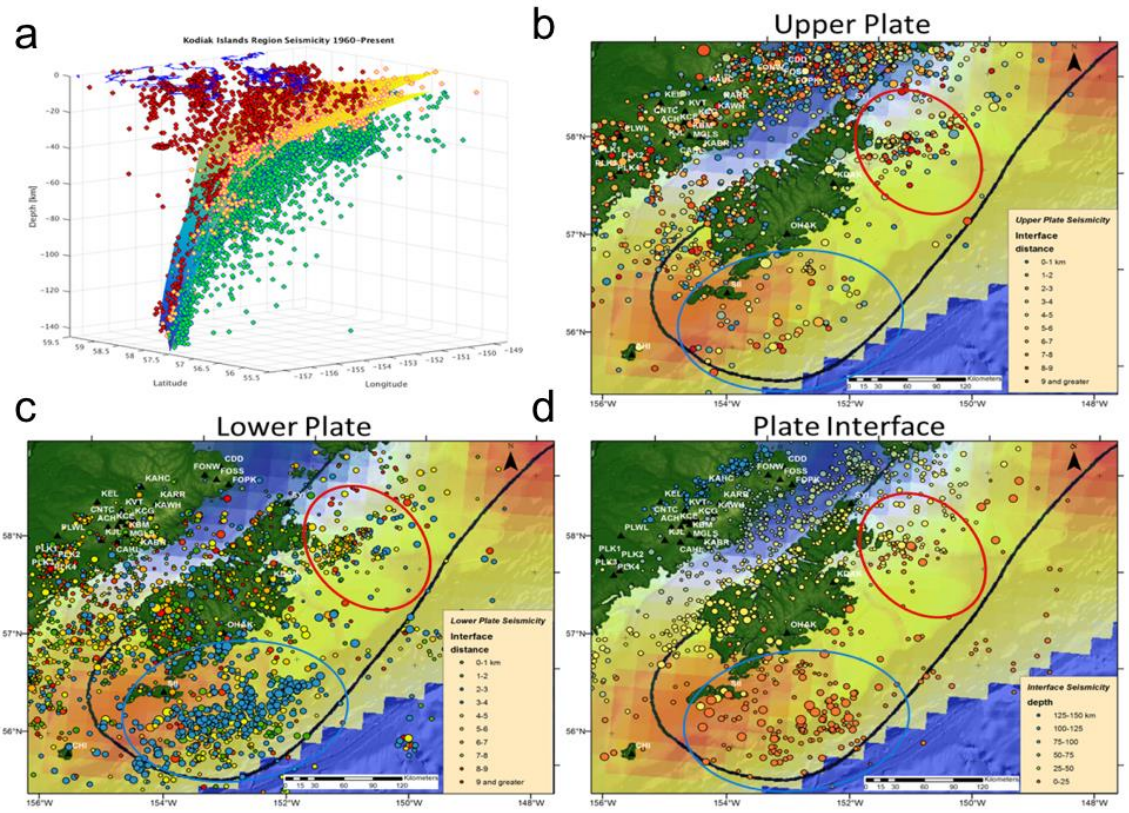

Figure 7. a) Wadati Benioff seismicity distinguishes the upper plate (red), interface (yellow), and lower plate (green) events in the vicinity of the Kodiak Islands. b) Upper plate events scaled by magnitude and colored by depth above the Slab1.0 plate interface c) Lower plate events scaled by magnitude and colored by depth below the Slab1.0 plate interface d) Interface events (+/- 10 km from the Slab1.0) scaled by magnitude. Orange patches correspond to highly locked plate interface regions and the thick black line approximates the 1964 aftershock zone (Zweck et al., 2002). Red circle denotes clusters of seismicity near the northeast Kodiak segment boundary and the blue circle denotes clusters near the southwest Kodiak segment boundary, mostly located seaward of the locked zone, on or below the megathrust.

Seismic reflection data

The former Mineral Management Services of Alaska (MMS) acquired airgun seismic reflection data across the entire Gulf of Alaska continental shelf (Figure 8). These legacy seismic data have been previously digitized, migrated, and CDP-stacked in the time-domain. I provide a structural interpretation of key MMS profiles that show evidence of faulting deduced from either scarp height (bathymetry) or high-density contrast (gravity). To complement the regions of the shelf where the MMS data do not

sample, I include legacy sparker seismic data acquired by the USGS and plate interface geometry with the EDGE dataset. The EDGE seismic line bisects the forearc in between the Kodiak Islands and the Kenai Peninsula and was the site of both multi-channel seismic reflection (Moore et al., 1991) and ocean-bottom seismometer refraction (Ye et al., 1997). The MGD77 database is shallow (< 200 m deep) legacy seismic sparker data. Seismic reflection data acquired by the USGS include several profiles along the continental slope and shelf (green lines in Figure 8) and can be used to understand shallow megathrust structure (von Huene et al., 1987).

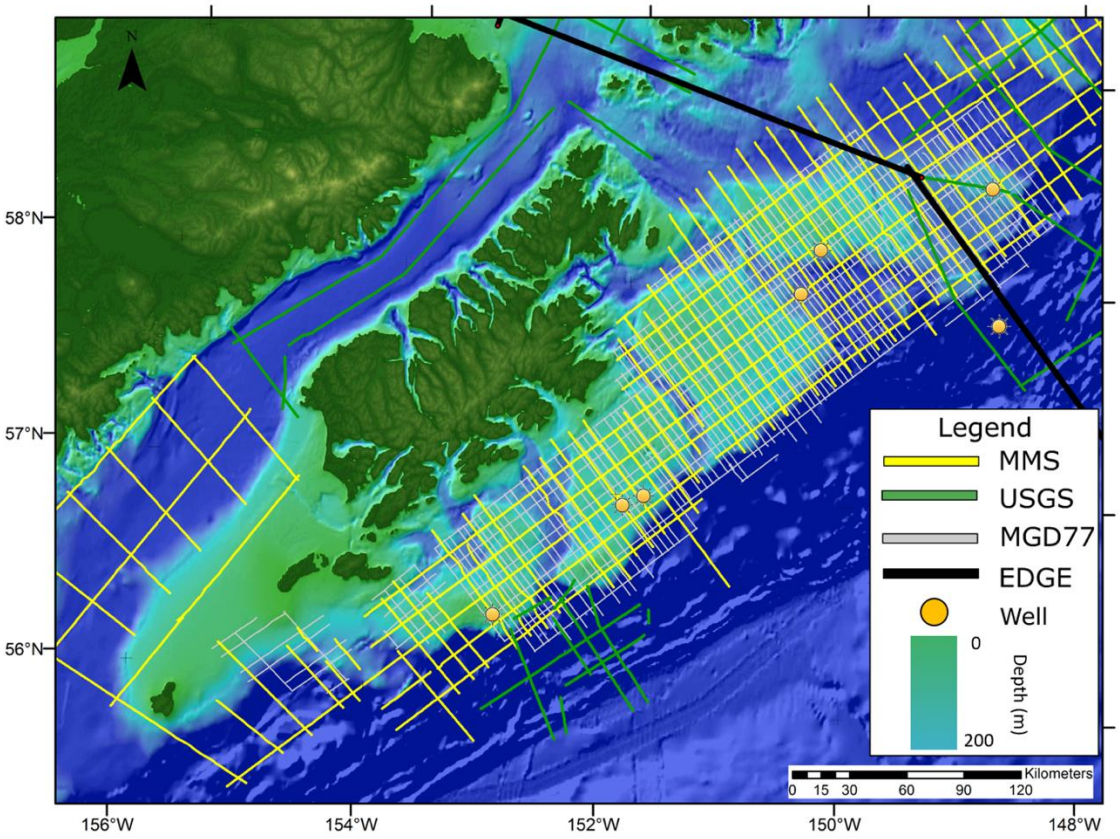

Figure 8. Bathymetry map of Kodiak Islands region showing location of several active-source seismic experiments. Yellow lines indicate Mineral Management Services track lines (MMS), green are USGS survey track lines, light grey are lease sale shallow sparker-source reflection track lines (MGD77), and black line is the crustal-scale transect across the shelf (EDGE) track line. Off-yellow circles denote borehole well

locations (Turner, 1987). The profiles of primary importance to this thesis are those located seaward of the Kodiak Islands, on the outer forearc and accretionary prism.

Tsunami Modelling

I compiled multi-beam bathymetry data for offshore Kodiak Island, which was accessed from the NOS Bathymetry grid database (2015/11/01, NOAA). The bathymetry data were gridded at one km spacing and converted to tsunami wave speed (v) in each cell using

$$v = \sqrt{gd} \qquad 9$$

where g is the acceleration of gravity (9.81 m/s^2) and d is water depth in meters (Lowrie, 2007). This relationship between tsunami wave velocity and ocean depth follows from the shallow gravity wave assumption and the condition that water depth is much less than the tsunami wavelength. The resultant velocity field was imported into the seismic processing software Promax™ for acoustic finite difference modeling of the tsunami wave-field (Figure 9).

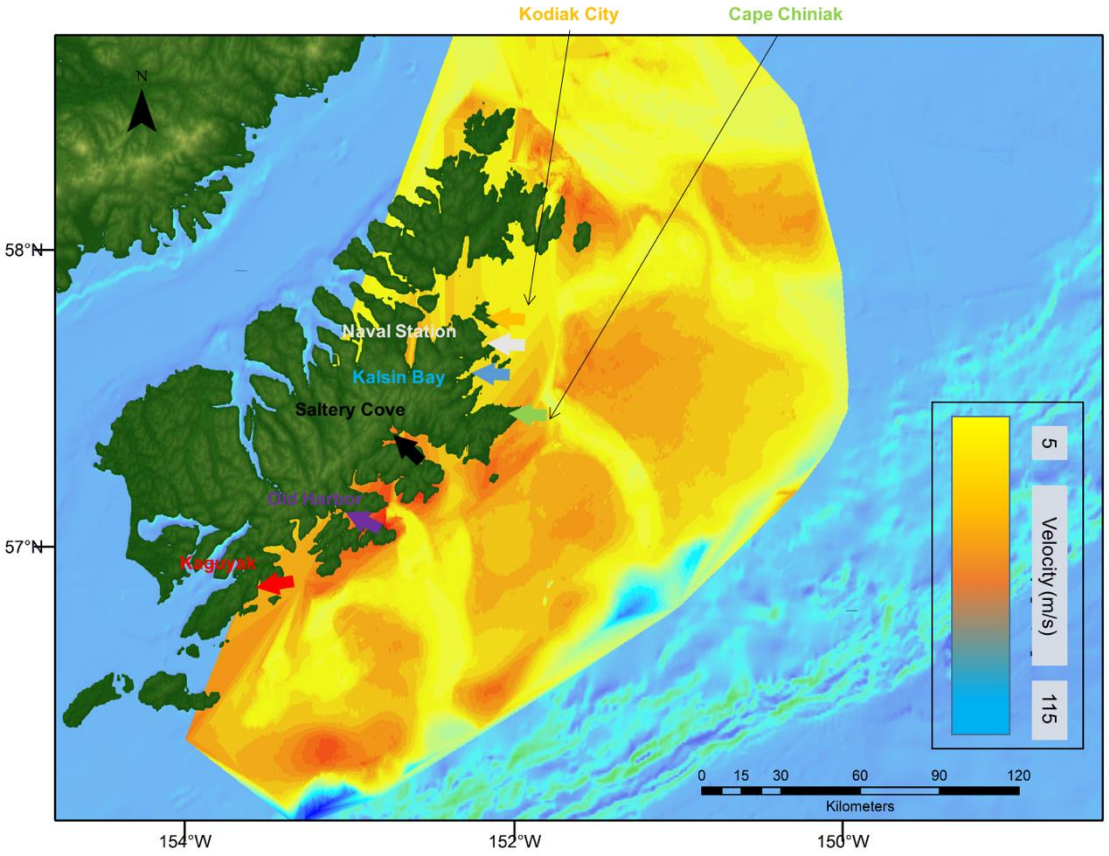

Figure 9 Tsunami velocity field (gridded at 1 km spacing), derived from NOAA water depth database. Each arrow corresponds to a tsunami run-up site on the Kodiak Islands and is color coded to represent its respective source.

Kaguyak, Old Harbor, Saltery Cove, Cape Chiniak, Kalsin Bay, Kodiak Naval Station, and Kodiak City comprise seven first-arrival tsunami run-up locations on Kodiak Island following the 1964 event (Table 2; Figure 9). Each run-up location was treated as a point source generation for tsunami waves and back-propagated in time using the reported travel times for each run-up location and water depths derived from the NOAA database. Travel times are defined as the onset time of the 1964 mainshock to the arrival time of the leading wave-crest onshore. The emanating wave-field is captured in one-minute time steps up until the total travel time for each respective source point onshore. The final time step for each modeled source represents the distance the wave traveled

based on the reported arrival times and estimated water depths. The first-arriving wave crest was then isolated and georeferenced in order to view the geospatial convergence of the multiple back-propagated sources.

Table 2.1 Tsunami travel times. Travel difference in the third column is taken to be the relative difference in time between the source convergence point (-152.715 W, 57.061 N) and the closest distance to each modeled wave-front. Table modified from Plafker, 1969.

Inundation Site	Travel Time (min)	Travel Difference (min)	First Motion (reported)
Kaguyak	38	6	NA
Old Harbor	48	24	Up
Cape Chiniak	38	0	Up
Kalsin Bay	70	13	NA
Naval Station	63	5	Up
Kodiak City	45	5	Down
Saltery Cove	30	0	NA

CHAPTER THREE: NORTHEAST KODIAK SEGMENT BOUNDARY

The rich morphology of the deep ocean floor is a direct consequence of the tectonic, sedimentologic, and volcanic processes that shape it. Seamounts, fracture zones, and varying amounts of sediments are present on the incoming Pacific plate offshore of the Kodiak Islands. Seamounts are submarine mountains that are built from hotspot volcanism, whereas fracture zones are the inactive, extensional remnant of a mid-ocean ridge system (Kennett, 1982). Large ridge and trough structures are a typical morphology of the fracture zones, and these remain structurally competent as they move away from the mid-ocean ridge, beneath varying amounts of sediment, and into the subduction zone (Menard and Atwater, 1969; Sandwell, 1984). Sediments that lie above volcanic basement offshore of the Kodiak Islands are mostly derived from eastern Alaska along the Surveyor Fan (Gulick et al., 2015).

Potential field, satellite topography, and bathymetry data provide key constraints on incoming and lower plate structure in the absence of sufficient crustal-scale seismic profiles across the shallowest regions of the trench (Sandwell et al., 2014). Marine gravity data help to uncover relationships between seismogenic behavior and variations in density within the upper plate (Song and Simons, 2003; Wells et al, 2003; Basset and Watts, 2015b). Magnetic field anomalies highlight variations in remnant magnetization and long wavelength (> 100 km) magnetic anomalies existing over subduction zones have been inferred to stem from mantle hydration or emplacement of mafic domains through episodic volcanism (Blakely et al., 2005; Saltus et al., 2007). Fracture zones

leave conspicuous offsets (from offset magnetic reversals) in otherwise continuous magnetic lineations that traverse the ocean floor, whereas seamounts are identified from circular magnetic anomalies.

An outstanding question concerns the fate of high-relief topography once it becomes subducted below the overriding upper plate. Incoming plate structure has been hypothesized to influence how megathrust ruptures nucleate or laterally arrest across the plate interface (Cloos, 1992; Bilek et al., 2003; Robinson and Watts, 2006; Wang and Bilek, 2011). Sediments also contribute to seafloor topography and must be accounted for in the subduction zone process. High erosion rates from the upper plate contribute additional sediment to a channel which exists between the upper and lower plates. Sediment channel volume can vary along-strike and influence the local plate coupling and thus the megathrust earthquake cycle (Heuret et al., 2012).

von Huene et al. (1999) inferred that the Kodiak-Bowie and Patton Murray seamount chains, and Aja and 58° fracture zones have influenced the rupture pattern of the 1964 Great Alaska Earthquake by both inhibiting rupture south of the Kodiak Islands and behaving as asperities, or local slip patches. These morphologies on the incoming Pacific plate have been subducting throughout the Cenozoic and their influence on the Kodiak segment earthquake cycle may leave behind distinct morphological and geophysical expressions within the accretionary prism and forearc. However, the geophysical signatures of subducted lower plate features are poorly characterized in the Kodiak Islands region.

The datasets I analyze to characterize the geophysical signature of the northeast Kodiak segment boundary are free-air gravity data and topography derived from satellite

altimetry, global magnetics grid EMAG2 (2-min arc resolution), the Harvard CMT catalog, and the USGS ANSS earthquake catalog for the Kodiak Islands (Dziewonski et al., 1981; Young et al., 1996; Maus, 2009; Sandwell et al., 2014) described in Chapter 2. I apply transformation techniques to the gravity field and utilize seafloor topography in conjunction with earthquake and focal mechanism data to provide a link between upper crustal tectonics and the N80W trending 58° fracture zone that is migrating beneath the Gulf of Alaska accretionary prism (Figure 10).

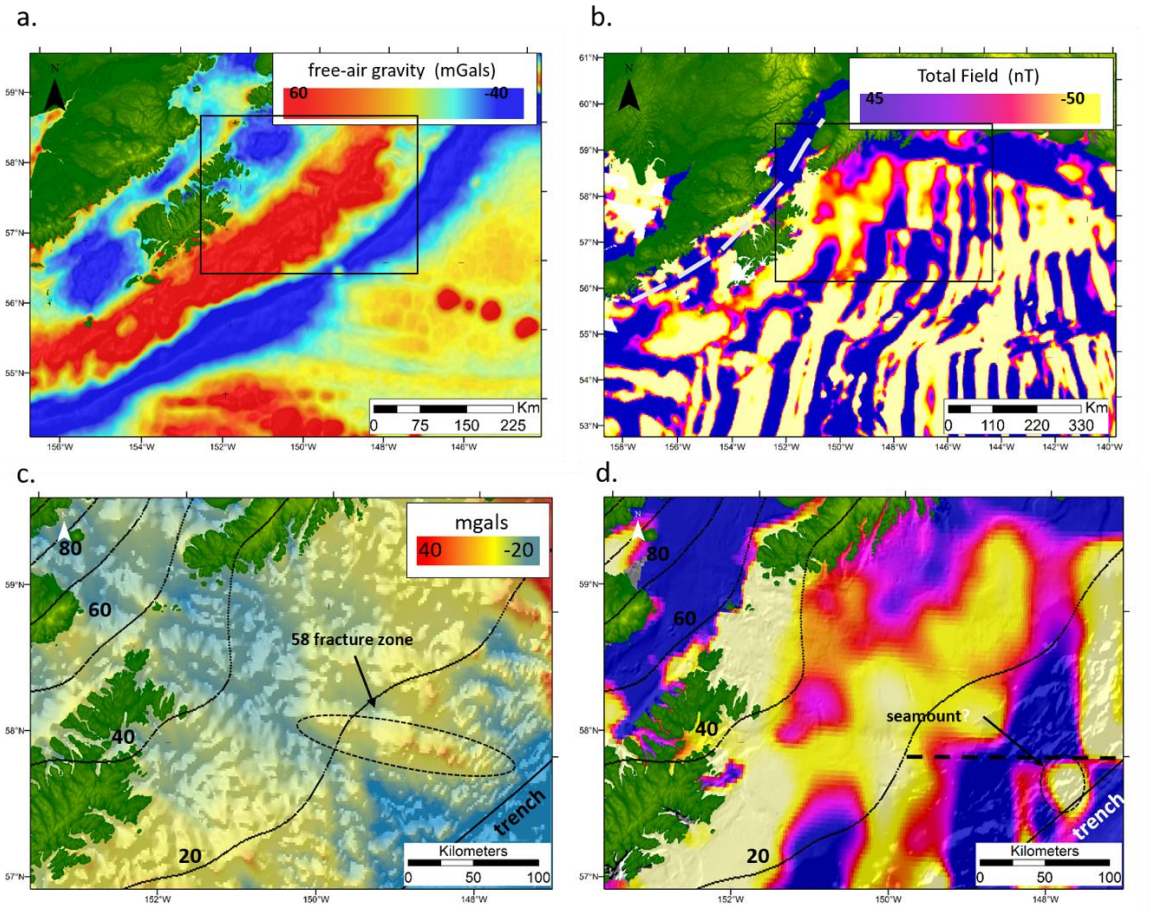

Figure 10. Potential field maps over the Kodiak Islands region, Alaska. Lower plots show zoomed in regions from the map directly above it. Clockwise starting from top left are the a) free-air gravity anomaly map, b) total magnetic fields (heavy dashed white line denotes the 570° C isotherm), c) upward-continued free-air gravity field to z = 3 km, and d) close-up of magnetic field. Note the E-W striking anomaly at approximately 58 degrees latitude present in both gravity and magnetics (dashed

black circle in c and dashed black line in d). Thin black lines in lower plots denote depth to plate interface in 20 km contour intervals (Hayes et al., 2012). The gravity expression of the subducted 58° fracture zone is a positive gravity anomaly below the accretionary prism (upward continued field) and it is imaged on the magnetics data as an offset lineament on the subducting Pacific plate.

Potential field signature of the 58° fracture zone

The 58° fracture zone does not show a strongly positive density contrast on the incoming Pacific plate due to a local sediment thickness on the order of ~2 km sitting at the trench axis (Reece et al., 2011). Figure 10a shows the free-air gravity anomaly map which captures the strong positive gravity anomalies from the seamount chains and Aja fracture zone, but not the 58° fracture zone as identified by von Huene et al. (1999). However, the total-field magnetic anomaly manifests the existence of the 58° fracture zone as a linear offset of magnetic stripes on incoming Pacific plate (Figure 10b).

I attenuate short-wavelength gravity-derived features using the upward continuation transformation to highlight long wave-length features below the forearc. (For explicit derivation of this transformation, see methods section in Chapter 2). I upward continue the pseudo-Bouguer gravity anomaly to a height of 3 km, after which a strong positive anomaly at approximately 58° latitude is revealed below the outer wedge (Figures 10c). This N80W lineament extends the subducted fracture zone beneath the outer wedge of the accretionary prism to approximately the edge of the continental shelf, but the lineation does not extend to beneath the inner wedge portion of the continental shelf. This suggests that either the fracture zone does not retain the same density character beneath the inner wedge, there may be a local thickening of sediments in the inner wedge that do not share the same positive gravity character, or that the gravity field data cannot adequately resolve the fracture zone below the strongly positive gravity

signature that dominates the Gulf of Alaska forearc. Along strike of this gravity high is a linear boundary separating low density materials from below the Kennedy Entrance from higher density materials beneath the Kodiak Islands. This muted lineation may represent the subducted fracture zone beneath the inner wedge that coincides with the boundary between Kodiak and Kenai subduction zone segments.

Total-magnetic field anomaly data show a lineation related to the 58° fracture zone that persists about 200 km landward of the trench axis, essentially beneath the outer wedge portion of the continental margin to a plate interface depth between 20 and 30 km (Figure 10d). Both the inner and outer wedges are comprised of accreted sedimentary terranes that have essentially no magnetic susceptibility, suggesting that this magnetic lineament is either consistent with a source from the subducting lower plate (Saltus et al., 2007) or an upper plate fracture zone influence. The Curie isotherm is estimated to reside ~260 km from the trench near the Kodiak Islands, at a plate interface depth of 55 km (Gutscher and Peacock, 2003). Since this isotherm lies inland of the northwest termination of the observed lineament (Figure 10d), thermal resetting of remnant magnetization is presumably not the driving factor for the subducted fracture zone limit.

Global subduction zone studies have discerned density or magnetic anomalies stemming from subducted structures such as seamount chains and ridges, and they have a clear expression below the forearc (Wells et al., 2003; Basset and Watts, 2015b). My results suggest density and magnetic susceptibility contrasts related to a subducting fracture zone can be imaged beneath the Kodiak forearc. Upward continuation provides a means to attenuate high-frequency gravity signals and for interpreting anomalies that owe their origin to deeper crustal sources. Assuming the lineation is sourced at or in proximity

to the megathrust boundary, the limit to characterizing the subducted 58° fracture zone appears to be approximately 50 km depth to the plate interface using both potential field datasets (Eberhart-Phillips et al., 2006). However, the trend of the gravity and magnetic lineations are consistent with the expected geophysical expression of subducting fracture zone.

I now compare the 58°fracture zone to coseismic (1964) and interseismic observations to constrain the tectonic role this structure has on the Alaska megathrust between the Kodiak and Kenai segments.

Interseismic observations

There is a relative paucity of large magnitude (Mw > 6) events from 1974 (start of modern catalog) to present for the northeast Kodiak Islands segment when compared to other portions of the Kodiak segment (Figure 11b). Available focal mechanism solutions for Mw 4.5-6 events show predominantly strike-slip oblique fault motion near 58° latitude (Harvard CMT catalog). These events all occur beneath the inner wedge east of the Kodiak Islands and along the presumed Kodiak segment boundary. Several of these strike-slip events have hypocenters within 10 km of the slab plate interface (Ye et al., 1997). The subducting 58° fracture zone might serve to facilitate strike-slip motion on faults across the plate boundary due to oblique subduction and first-order differences in how horizontal strain is partitioned across the fracture and upper plate contact (Lebrun et al., 1998). The observed focal mechanism character agrees with this model of fracture zone subduction and extends the limits of the fracture zone observed in potential field data. However, there exists an appreciable amount of Surveyor Fan sediment that has been subducting with the Pacific Plate since the Miocene and this has been imaged with

seismic profiles north of the Kodiak Islands below the outer wedge (Fruehn et al., 1999; Reece et al., 2011). The 58° fracture zone has been subducting longer than the addition of Surveyor sediment, so perhaps the strike-slip motion we observe today is a reactivation of a preferred stress field that was established during the longer time scale of fracture zone subduction (von Huene et al., 2012). Alternatively, the 58° fracture zone may be a leaky transform fault system which would have generated accessory ridges along strike of this fracture zone (von Huene et al., 1980). In this case, the observed strike-slip faulting mechanisms might be explained by a complex and heterogeneous fracture network engendered by subduction of high-relief topography (Wang and Bilek, 2011).

A number of small (m_L =< 4) earthquakes have occurred northeast of the Kodiak Islands (Figure 11b). Events within the upper plate (depth < 40 km) occurring post-1964 show a NE-SW spatial trend. This trend is shared by near-shore splay faults offshore Kodiak, which indicates active fault motion.

Plate coupling models suggest the southwest Kodiak region is strongly coupled (>0.8) to the Pacific plate and therefore locked and accumulating strain in the upper plate (Zweck et al., 2002; Suito and Freymueller, 2009). In contrast, the northeast segment shows lower geodetic coupling (0.2-0.6) and this coupling level persists across the adjacent Kenai segment (Figure 12). Geodetic inversions for plate locking suffer from non-uniqueness the farther GPS stations are from the trench, so the up-dip and lateral limit of megathrust locking is poorly resolved here. Figure 12 shows geodetically derived interseismic coupling and seismic, geodetic and tsunami-derived coseismic slip from

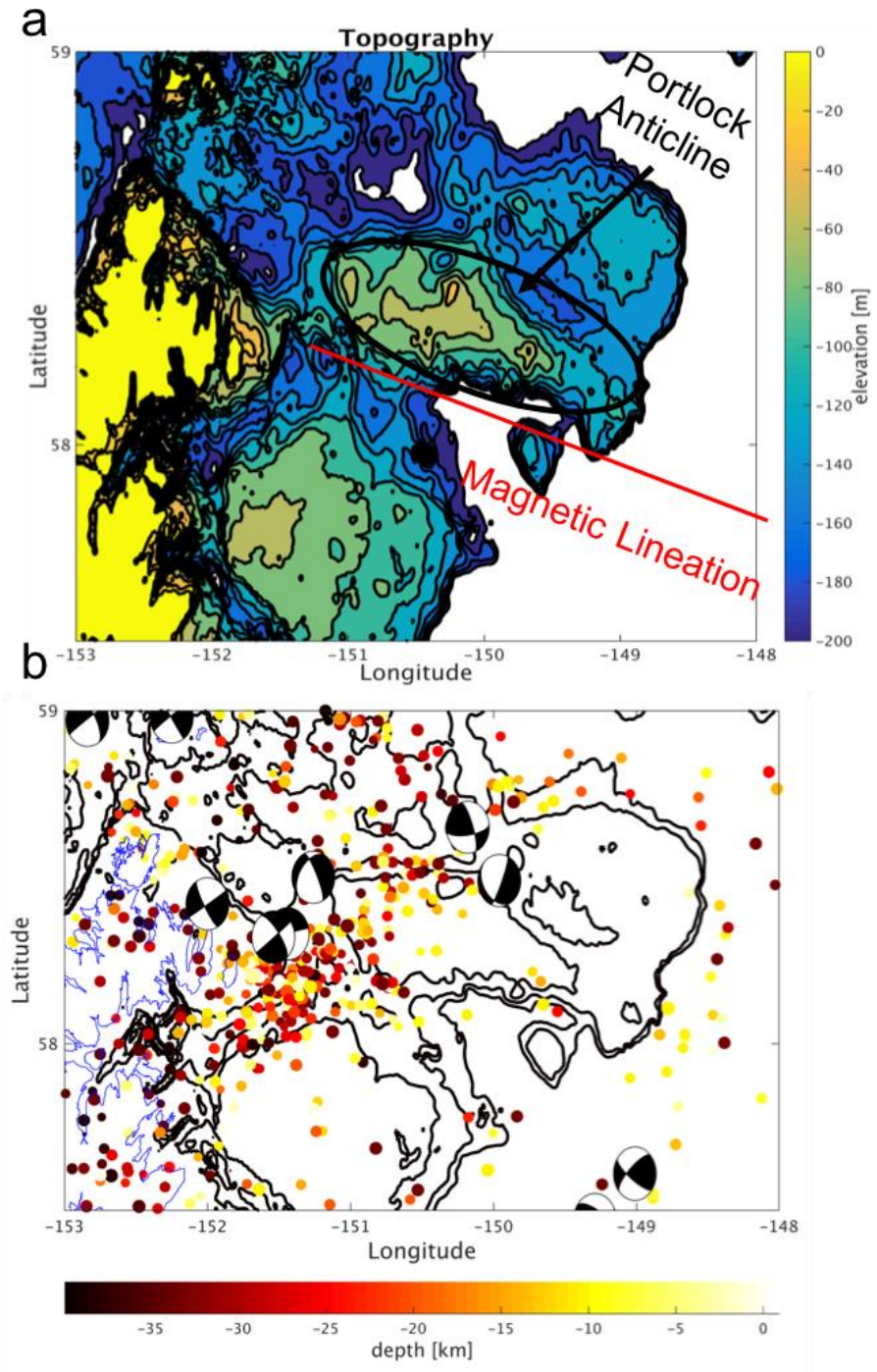

Figure 11. Satellite derived topography (Smith and Sandwell, 1997). Elevation is limited to above 200 m depth below sea level to accentuate shelf topography and the Portlock Anticline. The strike of the projected magnetic lineation indicative of the 58° fracture zone is highlighted in red and projects just south of the Anticline. b) compiled ANSS earthquake and Harvard CMT focal mechanism catalogs. Focal mechanisms show predominantly strike-slip fault motion (Mw > 4.5) with an oblique component. Local magnitude events are colored by depth and scaled by magnitude. A Gutenberg-

Richter relationship for these events is shown in the top right inset figure. Topgraphy is colored in black for spatial reference to a.

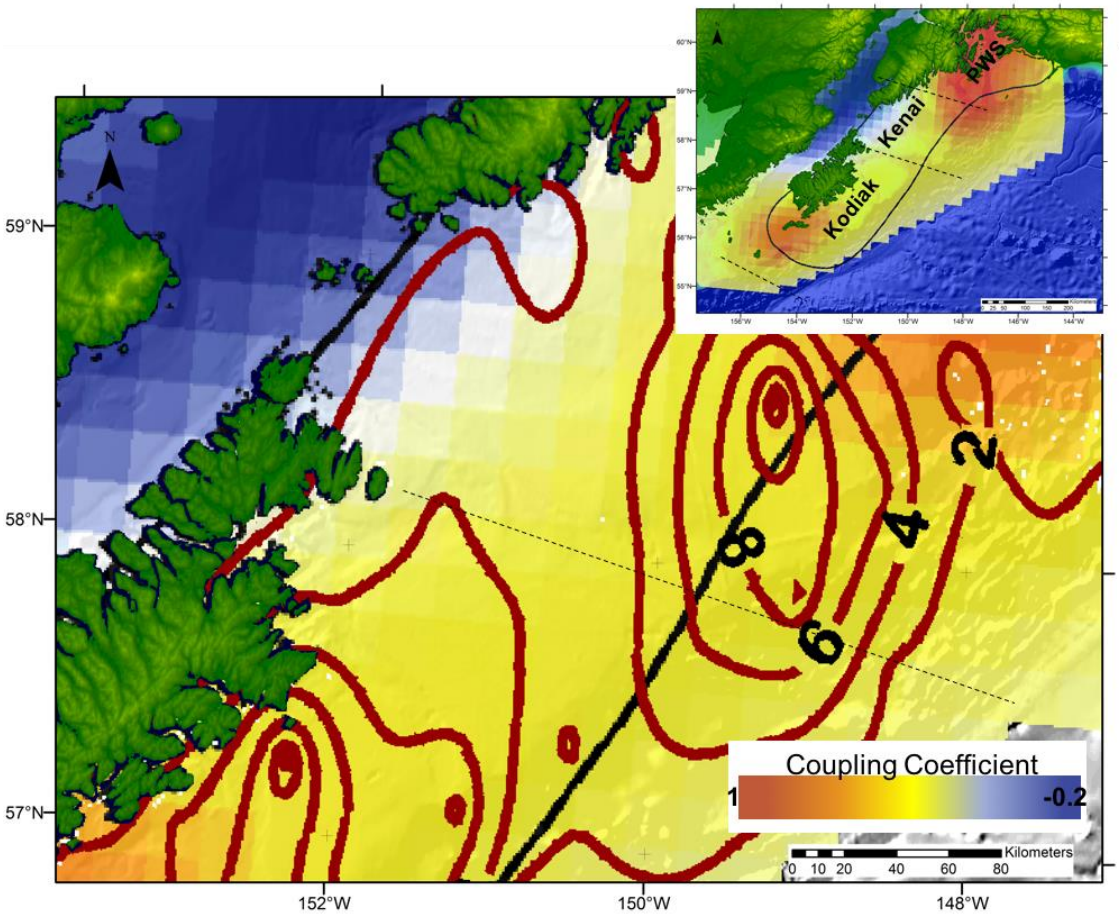

Figure 12. Interseismic coupling map (Zweck et al., 2002) and coseismic asperity distribution (Ichinose et al., 2007) for northeast Kodiak Islands region. Inset regional map shows the plate coupling across the Gulf of Alaska from the 1964 Great Alaska Earthquake. Warm colors correspond to highly locked regions. The dashed black line is the projection of the gravity and magnetic lineation interpreted as the 58° fracture zone. The fracture zone approximately separates the Kodiak and Kenai asperities but does not seem to influence the geodetic coupling on the Zweck et al. (2002) model.

1964 (Zweck et al., 2002; Ichinose et al., 2007). There is no modeled change in the interseismic plate coupling coefficient across the subducted fracture zone, which suggests the fracture zone either has minor influence on upper plate strain, or that the GPS data are not sensitive enough to resolve this deformation. The latter case is likely given that the nearest GPS station used in the Zweck et al. (2002) model is greater than 100 km from the E-W trending anomaly in the upward-continued gravity field, which is up-dip along the plate interface depth.

Upper plate structural expression

A major structural feature on the upper plate of the northeast Kodiak segment is the Portlock Anticline, which divides the Stevenson Basin into two sedimentary sub-basins, matches the orientation of the fracture zone, and is within 5 km south of the total magnetic field lineament (von Huene et al., 1980; Figure 13). The Portlock Anticline may owe its existence to a transfer of lower plate material to the upper plate, which in turn induces subsidence (Stevenson Basin) and uplift. A high-relief, low velocity zone was identified at ~12 km depth below the EDGE line and was interpreted as evidence for sediment underplating or seamount subduction (Ye et al., 1997). Additionally, Moore et al. (1991) imaged a series of arched reflectors along the EDGE profile and concluded that a significant exchange of underplated (or duplexed) sedimentary material may be responsible for Paleogene growth of the Kodiak margin. This underplated region lies immediately below the mapped Border Ranges fault, is along-strike (to the northwest) of the subducted 58° fracture zone and may be responsible for the formation of the Stevenson Basin and Portlock Anticline. While there is no structural high analogous to the Portlock Anticline mapped above the underplated body along EDGE, the fracture

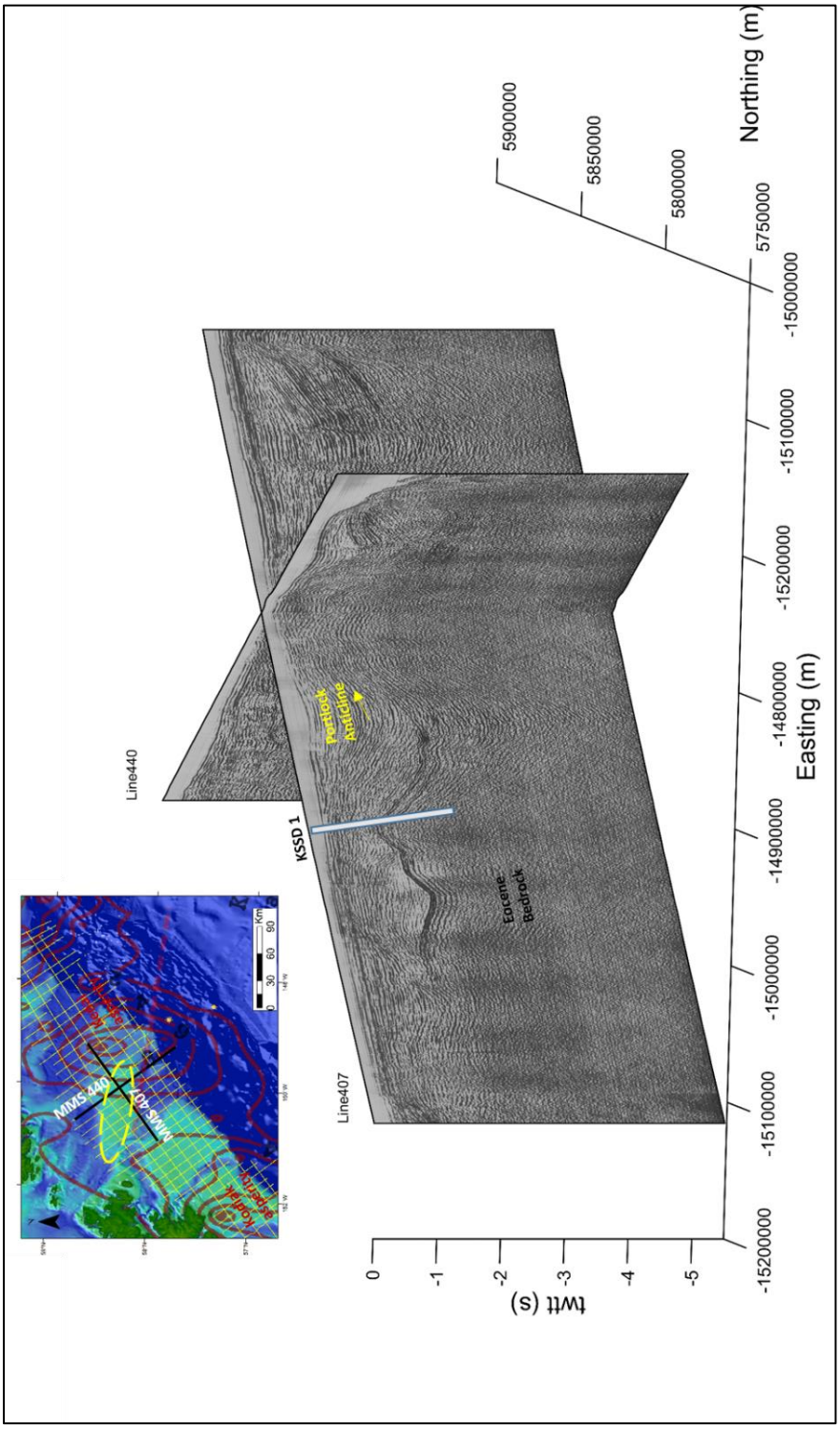

Figure 13. Upper plate structure above the subducting 58° fracture zone. The subsections of MMS strike line 440 and dip line 407 are denoted by the bold black lines. The Portlock Anticline is highlighted in yellow in both map and cross-section views. Geologic well KSSD 1 samples the upper 3 km of Stevenson Basin and provides lithologic control on line 407 (Turner, 1987). The magnetic lineation is denoted as the red dashed line on the inset map.

zone may provide sufficient mechanical control that is favorable to uplift at megathrust depths shallower than 20 km.

Persistence of the northeast segment boundary

In the context of the 1964 Great Alaska Earthquake, the 58° fracture zone did not behave as a boundary to rupture, although this feature separates significant slip between the Kodiak and Kenai asperities (Ichinose et al., 2007). Fracture zones involved in more recent megathrust ruptures did not serve to impede slip along the interface, but instead temporarily stalled it (Robinson and Watts, 2006). The Kodiak segment may have either ruptured alone or with the Semidi or Kenai segments in AD 1788 and AD 1430-1650 (Briggs et al., 2014; Kelsey et al., 2015). Given sparse geologic measurements that document previous upper plate motion, observations of interseismic deformation (i.e. seismic, geodetic) patterns coupled with longer timescales represented by subducting structure (i.e. from potential field observations) may shed more light on segmentation.

Segmentation models based on moving-window moment tensor stress inversion in this region of the Alaska megathrust conclude that first-order segmentation can be related to subducting fracture zones (Lu and Wyss, 1996). This is in agreement with the observed change in focal mechanism character across the Kodiak segment and the general lack of large earthquakes within the northeast segment relative to the southwest segment (see Chapter 5 for discussion of the southwest region). The mechanical role of fracture zones may be to locally reduce plate coupling across the interface and impact dynamic stress conditions in the megathrust earthquake cycle (Lu and Wyss, 1996). An updated segmentation model places a boundary in the middle of the Kodiak segment, but this

model does not take into account geomechanical controls from incoming plate morphology (Porto and Fitzenz, 2016).

A cross section perpendicular to the trench with nearby focal mechanisms projected along this line shows a possible model for how the fracture zone interacts with the upper plate (Figure 14). The nearby EDGE seismic line shows evidence for underplating of high-relief, low velocity material, which suggests underplating or seamount subduction (Moore et al., 1991; Ye et al., 1997). The 58° fracture zone is located just south of the EDGE line, and a similar tectonic process may be at work below northeast Kodiak.

Potential field data reveal the 58° fracture below the incoming plate, mostly beneath the outer wedge. Gravity data indicate this N80W trending anomaly that does not extend further than the continental shelf break, where the plate boundary depth exceeds 20 km depth. Magnetics data trace the geophysical signature of the fracture zone farther beneath the inner wedge. The upper plate response of the subducted fracture zone is structurally manifested by the Portlock Anticline. The 1964 earthquake suggests that slip was reduced along the subducted fracture zone and post-1964 seismicity suggests an interseismic stress field that is preferential to strike-slip oblique motion along the northeast Kodiak segment boundary. These moderate interseismic earthquake events may be the product of a subducting fracture zone coupled with differences in plate convergence and possible underplating.

Collectively, different geophysical datasets have been used in conjunction to trace the subducting 58° fracture zone, its structural manifestation on the upper plate, and how this feature may allow for the Kodiak segment to rupture independently of the Semidi,

Kenai, and PWS segments. This is the first study to bring together various geophysical data across northeastern Kodiak and proffer an updated seismotectonic framework for this segment boundary.

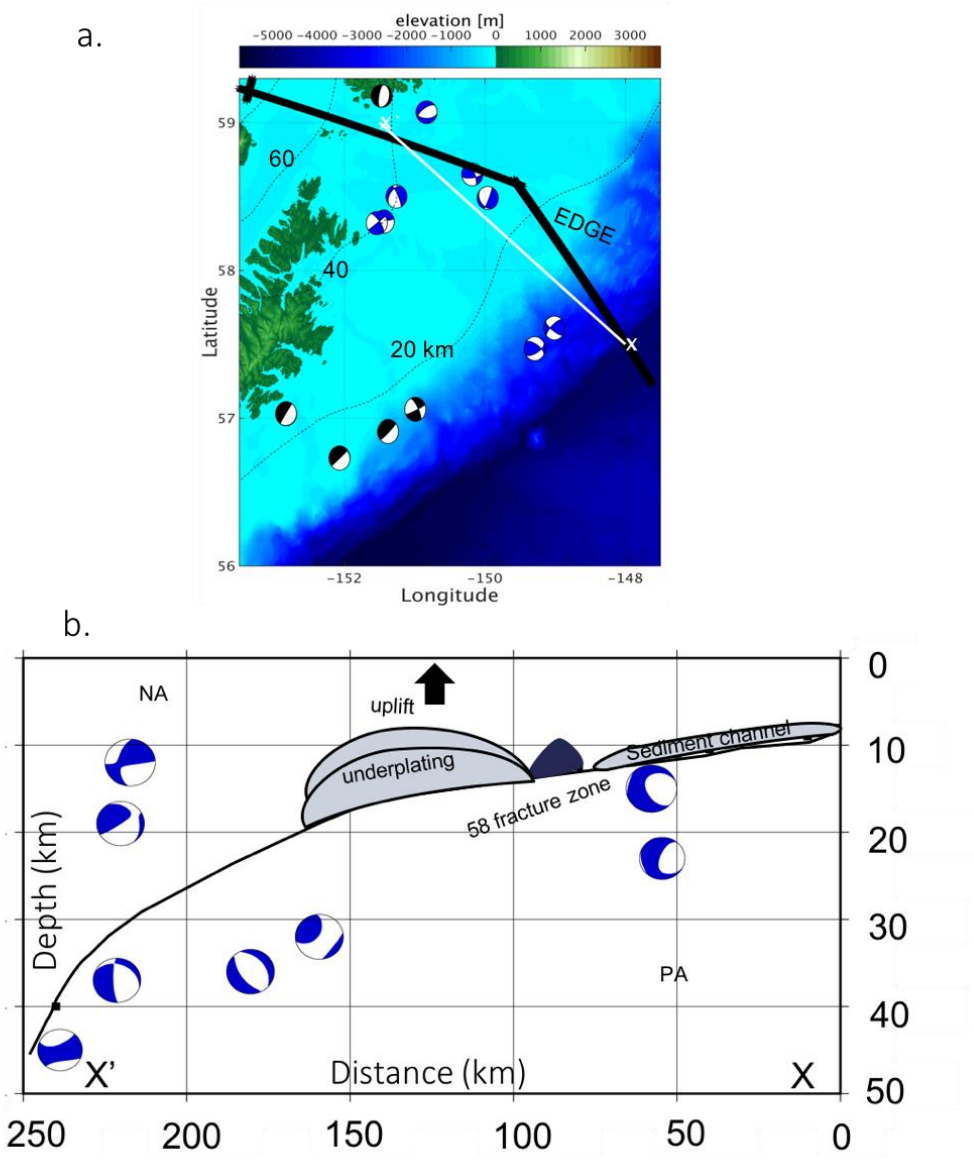

Figure 14. Hypothesized model for subduction of the 58° fracture zone. a) map view of northeast Kodiak region with overlain focal mechanisms. X-X' denotes cross section in bottom figure. b) cross section across trench with nearest neighbor (50 km) Harvard CMT focal mechanisms projected onto it. Megathrust geometry (black line) is constructed from two plate models: interface depths shallower than 20 km are constrained from the EDGE line 302 (Ye et al., 1997) whereas depths greater than 20 km are from the Slab1.0 plate model (Hayes et al., 2012). Grey polygon is a high-relief structure that may be associated with the subducting fracture zone. Sediment channel is shaded in grey and drawn above subducting Pacific Plate (exaggerated scale). Suspected underplating of these sediments may be occurring somewhere in front of the fracture zone.

CHAPTER FOUR: TSUNAMIGENIC FAULTS OF THE KODIAK SEGMENT

The M9.2 1964 earthquake engendered a local tsunami that inundated several onshore locations spanning the Kodiak Islands. Initial estimates of potential tsunamigenic sources suggest any fault system located between Montague Island and offshore Kodiak could have generated the observed first arriving wave-crests (Plafker, 1969).

During megathrust earthquakes, elastic strain accumulated on the upper plate is released (uplift or subsidence) as the seismogenic region (plate interface) slips. Previous models have attempted to constrain the slip-distribution along the plate interface and its relationship to splay fault coseismic uplift during the 1964 event. Johnson et al. (1996) conducted an inversion of tsunami and geodetic data, and their results suggested three primary regions of focused slip at the interface, the PWS and Kodiak asperities. In their model, the Kodiak asperity is located immediately east of the Kodiak Islands and experienced 10-15 m of slip towards the shallower region of the seismogenic zone (Figure 15).

In contrast to the Johnson et al. (1996) model, a joint inversion of tsunami, geodetic, and earthquake data estimated 10 m of slip for the Kodiak asperity and in a slightly different location below the Kodiak segment (Ichinose et al., 2007; Figure 15). This model used a grid spacing of 50 km and constrained more slip towards the central Kodiak segment, extending below the Albatross Basin to the trench. The relationship between interface slip and seafloor uplift is variable across subduction zones. It has been observed that slip along a megathrust splay (termed the megasplay) faults are more conducive to

tsunamigenic behavior compared to motion along the frontal décollement (Moore et al., 2007). Splay faults that moved in response to slip along the PWS asperity were driven by

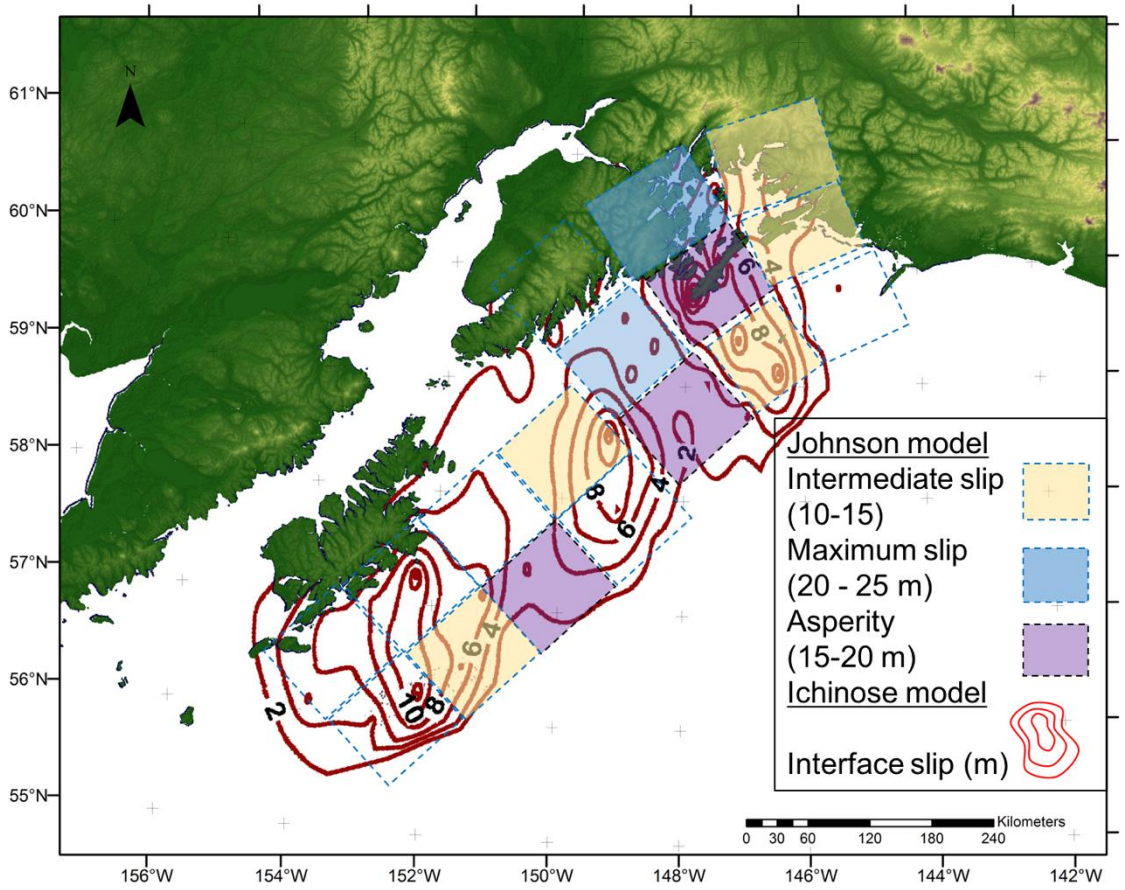

Figure 15. Comparison of two source models for interface slip/asperity distribution for the 1964 Great Alaska Earthquake. Ichinose et al. (2007) model is based off seismic, geodetic, and tsunami data while the Johnson et al. (1996) uses only geodetic and tsunami data. Slip patches in Johnson model are on the order of 100 km. Note that both models resolve three regions of focused slip and are generally in the same neighborhood. Figure adapted from Johnson et al. (1996) and Ichinose et al. (2007).

duplexing and material underplating (Liberty et al., 2013; Haeussler et al., 2015). The geometry of the Kodiak asperity from the two asperity models suggests splay fault

motion should be concentrated immediately seaward of the region of largest slip, assuming near vertical thrust faults (Johnson et al., 1996; Ichinose et al., 2007).

Inundation mapping of tsunami waves depend strongly on the length and magnitude of vertical uplift. Coseismic seafloor uplift calculated from interface slip is often used as an initial condition to numerical tsunami wave studies. It has been shown that the maximum tsunami run-up distance for sites on Kodiak Island can be closely matched with a complex tsunamigenic source model possessing several patches of slip along the megathrust (Sulemani et al., 2003). However, these source model results do not consider the scenario of a near-shore tsunami hazard and only resolve the long-wavelength (~100 km) uplift distribution.

In this study, I provide an independent constraint on the potential tsunamigenic source region through first-arrival time tsunami modelling and detailed bathymetry data that does not assume an a-priori megathrust slip pattern through geodetic or seismic constraints. I also characterize fault geometry in the tsunamigenic region and provide an updated tectonic interpretation of 1964 motion from my tsunami modelling results and from previously published observations for onshore motion (Carver et al., 2008; Carver and Plafker, 2008).

Tsunami modelling from the 1964 earthquake

Seven documented tsunami run-up locations on the Kodiak Islands have travel times measured from onset of the main-shock to first arriving wave crest (Plafker, 1969; Table 2). The reported travel times have inherent error as several sources were from eye-witness accounts. The reported sense of motions of the first-wave (up/down) exist for several run-up sites but were not used in the modeling exercise I conducted. First sense of

motion of all but one station (Kodiak City) of the first-wave arrivals were up, consistent with Kodiak Islands located landward of the hanging wall of the thrust fault(s) that potentially moved in 1964. I calculated the tsunami wave velocity from 1 km gridded bathymetry data in order to propagate each wave-front to its maximum spatial extent offshore based on reported travel times (see Methods, Chapter 1) where shallower water depths translate to slower tsunami travel times. The greatest depths along the continental shelf are about 200 m and correspond to glacial troughs (Kaufman and Manley, 2004). Thus, the maximum tsunami wave velocity is ~ 44 m/s and the average velocity is 28 m/s, corresponding to an average water depth along the shelf of 79 m.

Each wave-field is color coded to represent its respective run-up location onshore of the Kodiak Islands (Figure 16). Wave-fields spanning a larger extent correspond to longer reported first arrival travel times. My modeled results show that there is wave-field convergence for five of the seven run-up locations: Kaguyak, Saltery Cove, Cape Chiniak, Kalsin Bay, and Kodiak City (Figure 16). This region of convergence lies offshore Sitkalidak Island where a conspicuous seafloor fault scarp is coincident with the convergence of tsunamigenic sources. Based on published travel times, wave-fronts for Kalsin Bay (stream gage) and Old Harbor (personal account) do not converge at the same source region (Table 2, Chapter 1).

There are two possible explanations for this discrepancy. Either the documented arrival time is off by 13 minutes at the Kalsin Bay site and off by 24 minutes for Old Harbor observation, or there is more than one (first arrival) tsunami source. Given the inherent error in reported total travel times tabulated from Plafker (1969) and the velocity gradients present in the ocean bottom topography that I modeled, the Kalsin Bay travel

time could potentially be sourced somewhere other than offshore Sitkalidak Island. The Old Harbor model results suggests a further offshore source region, as its wave-front extends to both the southern offshore limit of the Narrow Cape fault (NCF) and the Albatross Banks fault zone (ABfz). This could suggest bimodal splay fault rupture in 1964 or an incorrect timing for the first wave crest. In addition, some of the wave-fronts from Kaguyak, Old Harbor, and Kalsin Bay achieve a secondary wave-field convergence towards the Albatross Banks region, and this may indicate a potential tsunami source from the fault system there (Figure 16). It should be noted the reported travel times

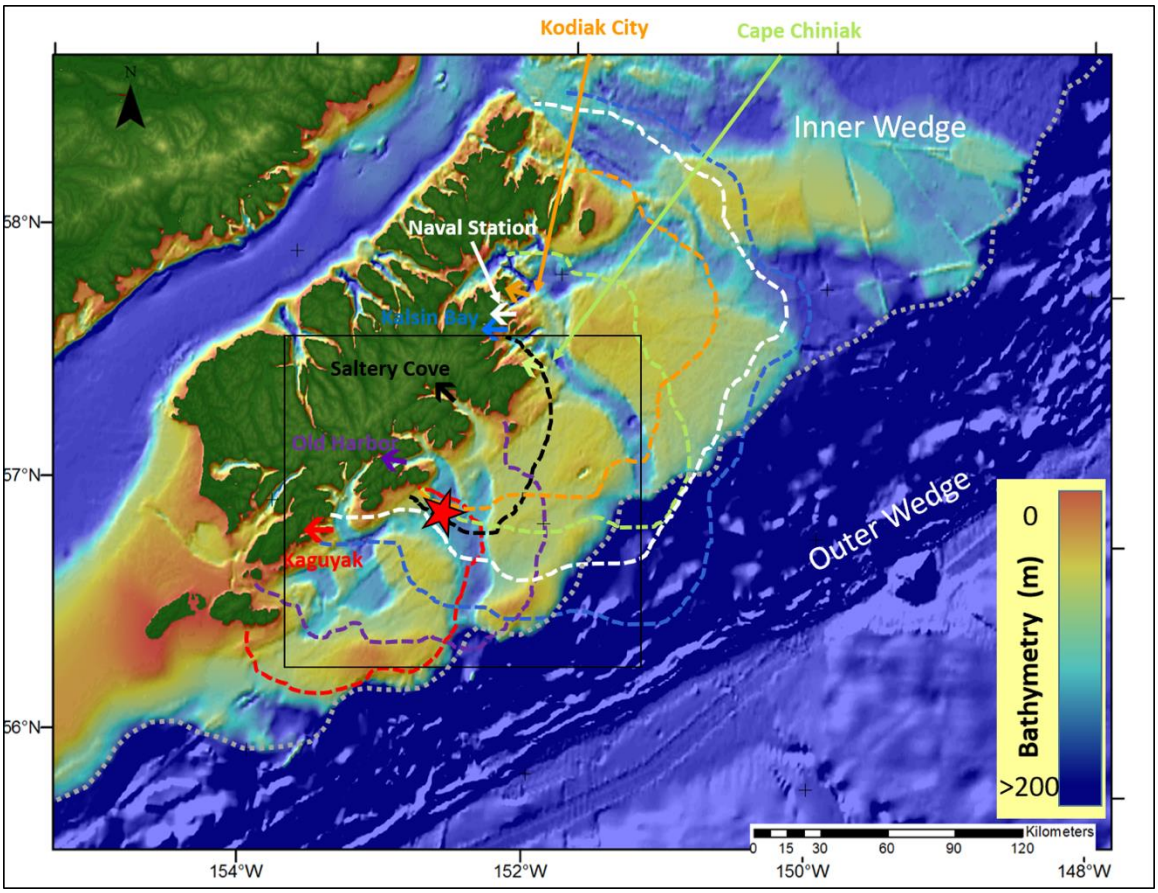

Figure 16. Finite difference modeling of tsunamis using a velocity grid derived from bathymetry. Each isolated wave-front is color-coded and labeled to correspond to its respective tsunami run-up site (Plafker, 1969). The outlined box is a close-up of the tsunamigenic source region where the red start indicates the convergence of five out of seven tsunami wave-fronts. The dashed gray line delineates the continental

shelf break. Black line denotes a close-up of the tsunamigenic source region shown in Figure 17.

account for only the first-arriving wave crest and thus does not preclude a second tsunamigenic fault source that could have induced a later arriving tsunami.

Tsunamigenic sources

There are two identified submarine fault zones offshore Kodiak that could have slipped in 1964. The northeast-trending ABfz is associated with a fold and thrust belt system within the forearc basin system that spans the continental shelf (Fisher and von Huene, 1980; von Huene et al., 1980). The KSfz parallels the ABfz, but is located immediately south of the Kodiak Islands and contains a number of linear scarps observed in the bathymetry that are mapped as faults (von Huene et al., 1980) and related faults that surface on the Kodiak Islands (Carver et al., 2008). Figure 16 shows a close up of the source region based off the back-propagated tsunami wave-fronts. The primary fault scarp associated with the KSfz is a conspicuous bathymetric lineament of the seafloor (Figure 16). Several MMS reflection profiles sample along-strike of the KSfz, which is situated 15 km offshore of Sitkalidak Island (Figure 17).

Reflector offsets in the MMS reflection profiles reveal distinct fault plane reflectors that span the tsunamigenic source region. Pre-1964 bathymetry (https://maps.ngdc.noaa.gov/viewers/bathymetry/, 2015/11/01) over each seismic line shows the changing seafloor topography. Offset reflectors, coupled with a bathymetric lineation suggests that seafloor topography is tectonically controlled. Therefore, prominent fault scarps associated with the KSfz are imaged on the northwest limit of MMS lines 476 through 492 (Figure 18). These seismic lines span 50 km along-strike of the KSfz and document differences in scarp height which may support an oblique

component to dominantly dip-slip fault rupture behavior and this is consistent with other studies (Carver et al., 2008).

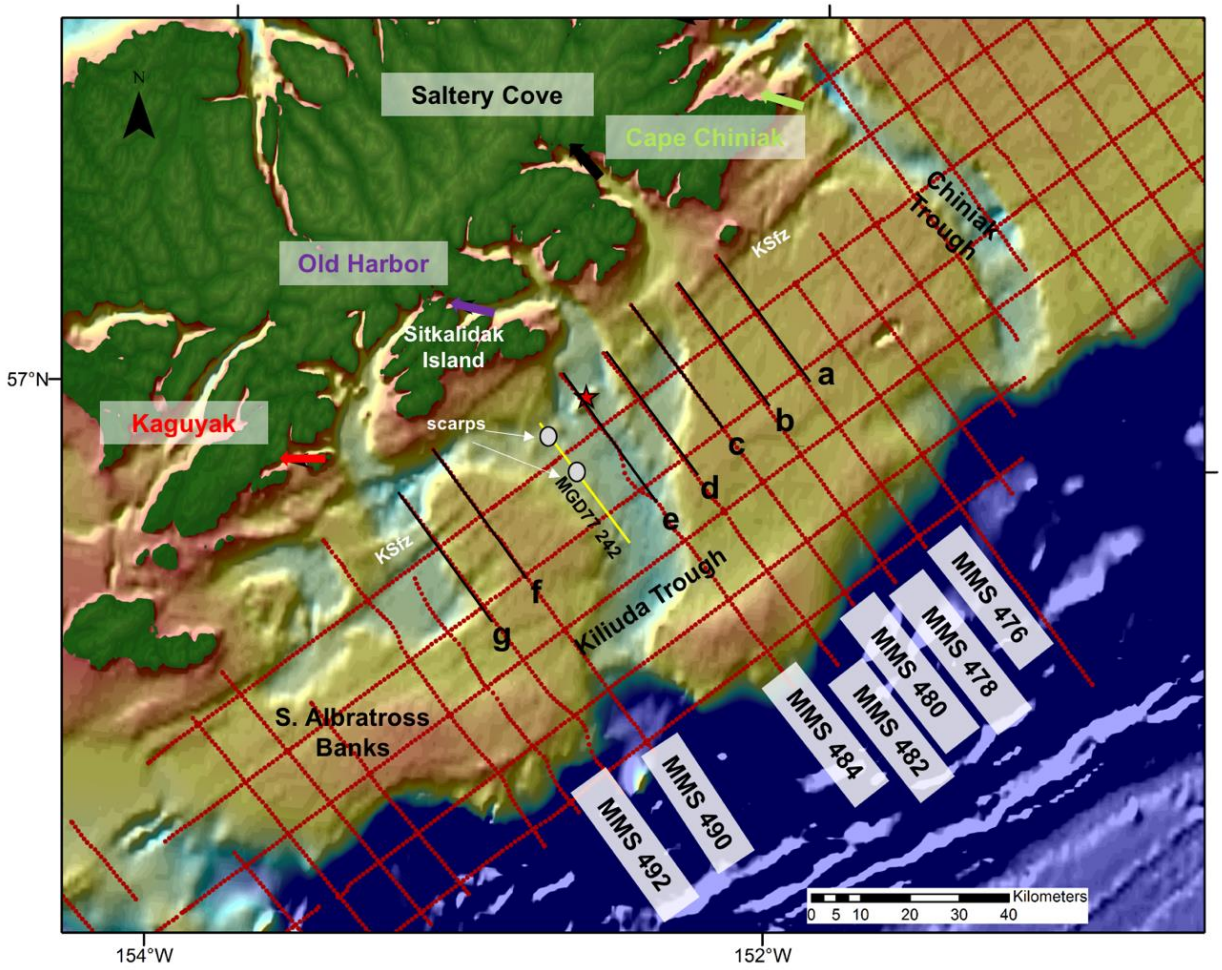

Figure 17. Close-up of the tsunamigenic source region. Red star is same as in Figure 16. Major structural features on the Kodiak continental shelf are labeled. Six MMS profiles that sample the KSfz are labeled and the northern most 30 km of these profiles are shown in Figure 18 a-g. Seismic sparker line MGD77 242 (in yellow) is highlighted in Figure 19. The two significant fault scarps imaged on the sparker line 242 (hanging wall up) are denoted by the white dots.

The faulting style that I interpret from offset reflectors of MMS lines 478, 480, and 484 is indicative of a keystone style horst accommodated by shallow fault branching from a primary mega-splay (Figure 18). Sparker seismic profile 242 shows a more detailed picture of scarp morphology in between MMS lines 484 and 490 (Figure 19).

The KSfz related scarp on profile 242 has very little ponding of Holocene sediment in the fault footwall, which implies a low rate of sediment deposition. This morphology is consistent with tsunamigenic splay faults near PWS faults observed near PWS (Liberty et al., 2013). MMS 476 shows at least two distinct faults which may control the 40 m topographic high seen on the corresponding bathymetry profile. MMS 482 is a little more difficult to interpret, but given a similar faulting style imaged on adjacent MMS profiles and the > 30 m relief shown on the bathymetry profile, there probably exists at least one mega-splay/antithetic fault pair that produces uplift. MMS lines 490 and 492 are located 20 km to the southwest from the other seismic profiles and shows a seaward-step in the KSfz, consistent with several other studies (von Huene et al., 1980; Fisher and von Huene, 1980). During the last glacial maxima (LGM), glaciers extended to the present day continental shelf offshore of the Kodiak Islands (Kaufman and Manley, 2004). The prevailing assumption is that under this significant ice load and subsequent ice scour, the seafloor surface was essentially reset; any significant seafloor topography observed today is all post-LGM (Carver et al., 2008; Liberty et al., 2013). Thus, faults scarps producing

offsets on the seafloor represent significant Holocene motion accommodated over multiple megathrust

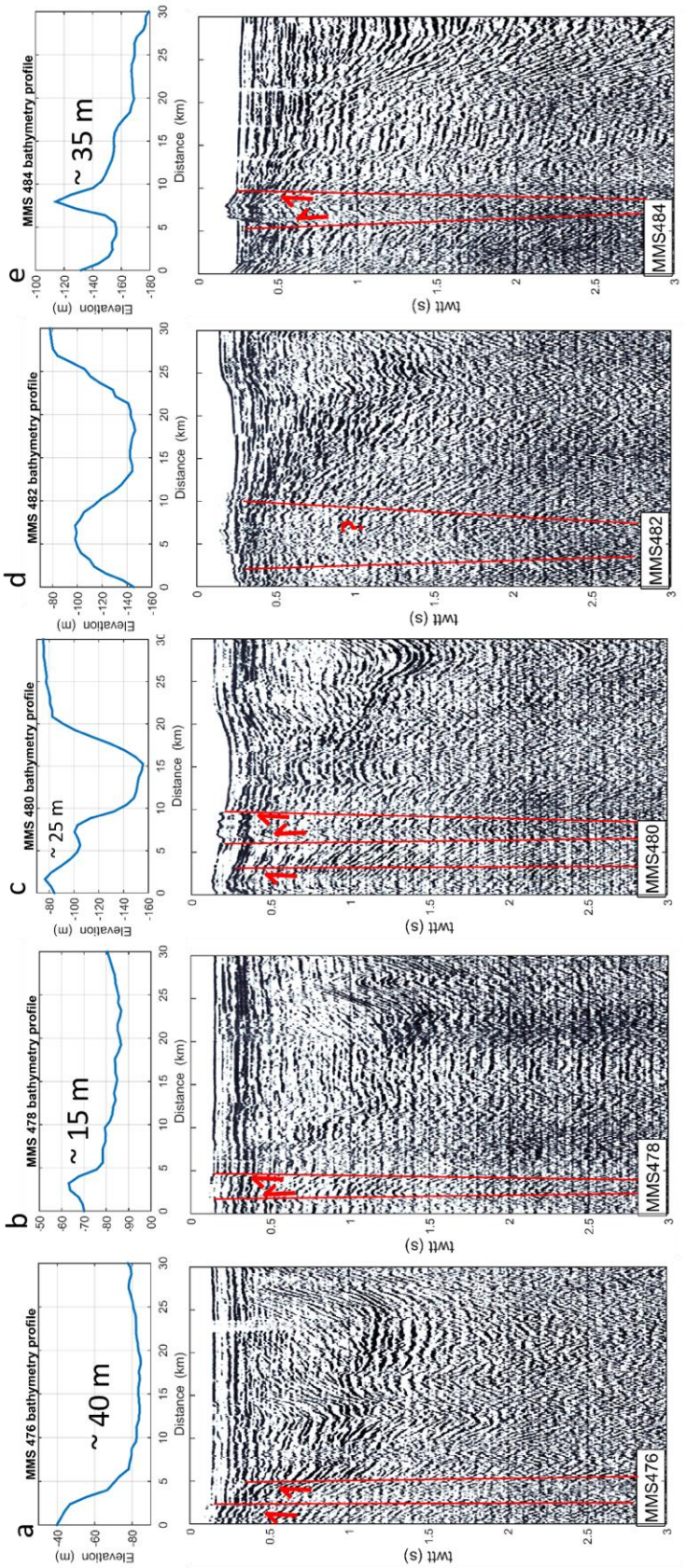
a
MMS 476 bathymetry profile
~ 40 m
Elevation (m)
Distance (km)
MMS476
1
twtt (s)
b
MMS 478 bathymetry profile
~ 15 m
Elevation (m)
Distance (km)
MMS478
1
twtt (s)
c
MMS 480 bathymetry profile
~ 25 m
Elevation (m)
Distance (km)
MMS480
1
2
twtt (s)
d
MMS 482 bathymetry profile
Elevation (m)
Distance (km)
MMS482
2
twtt (s)
e
MMS 484 bathymetry profile
~ 35 m
Elevation (m)
Distance (km)
MMS484
1
twtt (s)

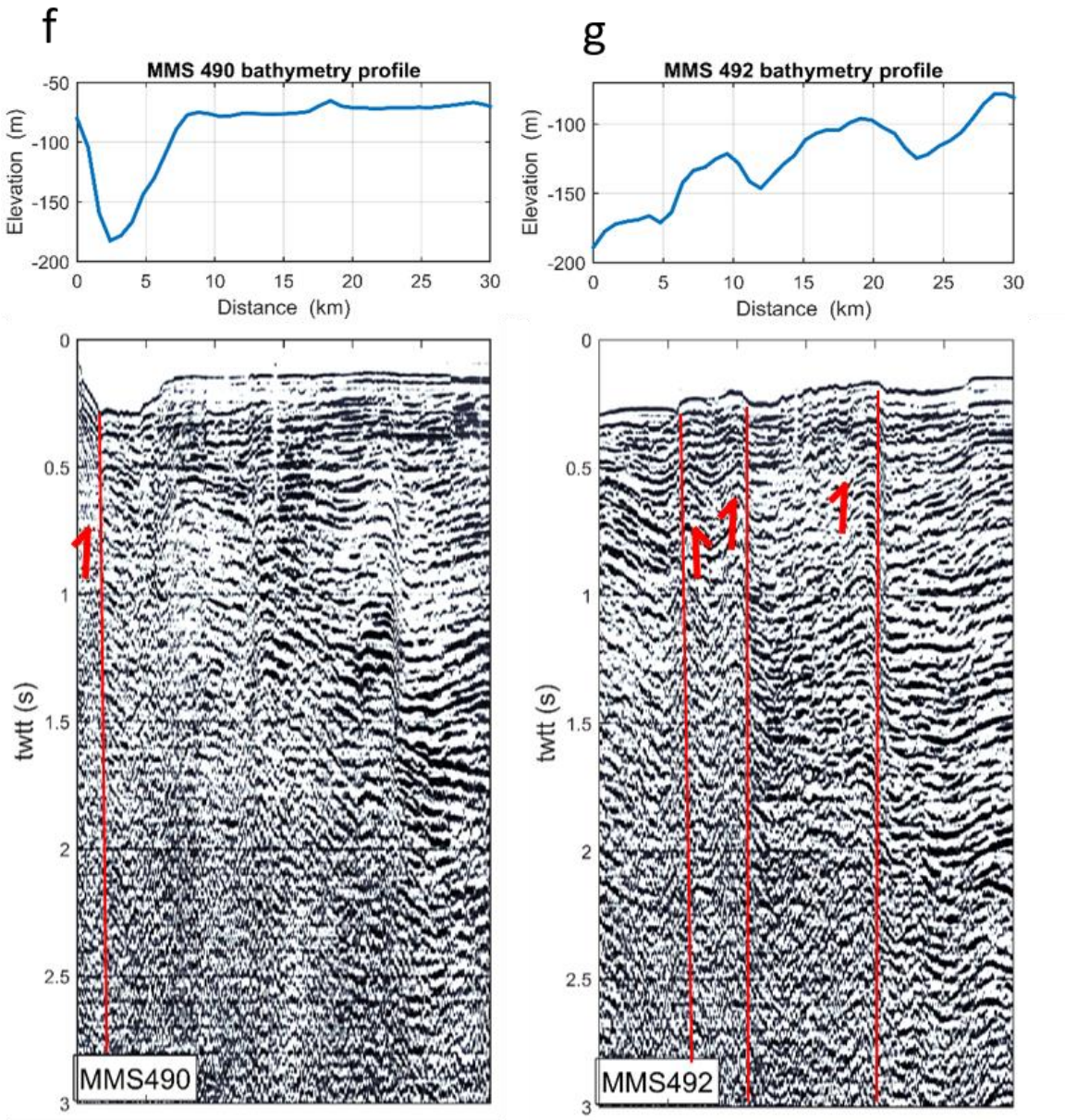

Figure 18. Interpreted MMS seismic reflection profiles that span the KSfz. Note that on all profiles, only the upper 6 km (3 seconds twtt) and westernmost profiles (30 km distance) are displayed to highlight the fault scarp associated with the KSfz. Primary faults related to the KSfz are interpreted by the bold red lines. Subfigures a-e are equidistantly spaced 10 km from each other. These MMS lines show the keystone graben type geometry of the splay faults. Profiles f and g are located 20 km south of a-e and show that the seaward-stepping behavior of the KSfz. Note that all seismic profiles are vertically exaggerated at 5:1. Bathymetric profiles are overlain on each MMS profile to highlight variation in fault-controlled seafloor topography.

earthquake cycles. It is unknown and not possible to discern whether all splay fault motion along the KSfz is the result of coseismic motion from 1964-like ruptures (multi-segment), or from rupture of the Kodiak segment alone. But assuming a recurrence interval of 500 years for the Kodiak segment, then in the ~12 ka time since LGM ice recession, the Kodiak segment has seen about 20 megathrust earthquake cycles (Carver and Plafker, 2008). Each identified fault scarp is equal to or in excess of 15 m and therefore a minimum slip-rate of ~1 mm/yr can be assigned to this region of the KSfz.

Tsunamigenic fault hazards for the Kodiak segment

From a seismic hazard perspective, it is important to stress the along-strike variability observed in scarp height, and thus in slip rates associated with the KSfz. It reinforces the idea that discrete and focused regions of this fault coseismically rupture while the remainder of the fault zone may experience very little to no coseismic motion. For example, paleoseismic investigations of the on-shore portion of the KSfz suggest no motion in 1964 (Carver et al., 2008). The preferred local tsunami source region that I model suggests a near-field tsunamigenic fault one within the inner wedge. Most of the back-propagated models converge to a narrow region of the KSfz and as both crustal-scale seismic reflection data and bathymetry data show, there are tremendous differences in how this fault zone has uplifted over the Kodiak segment earthquake cycle.

As mentioned before, the ABfz is another potential local tsunami source. This fault zone has an equal risk to coastal populations on the Kodiak Islands; though a resulting tsunami wave travel time would take a longer time to impact the shore from the ABfz when compared to the KSfz. Although high resolution bathymetry is not available for much of the ABfz system, a sparker profile shows sea floor offsets of more than 15

meters for this fault system, identical to scarp heights observed along the KSfz (Figure 19). Given that glaciation extended to the edge of the continental shelf and seafloor topography was likely reset during the LGM across the ABfz, motion across the

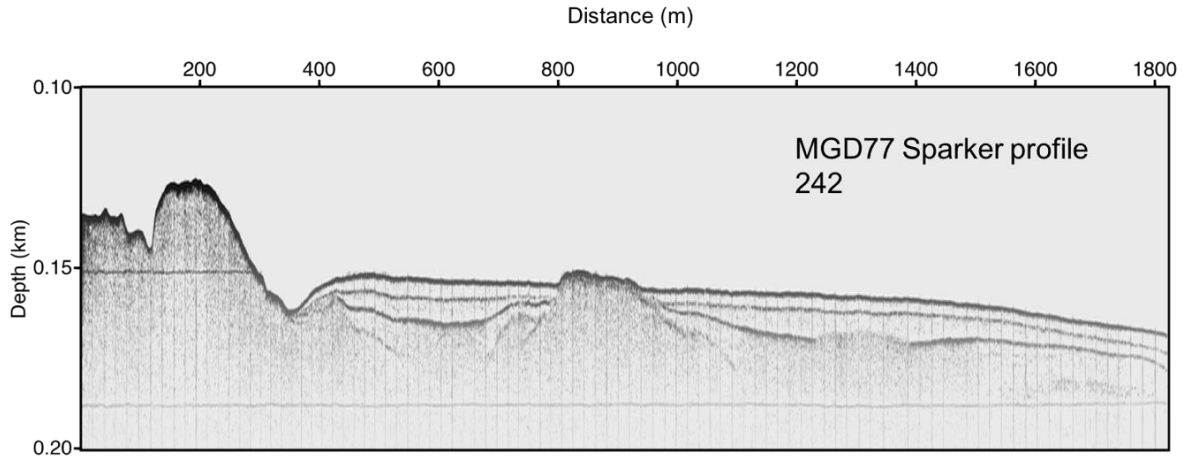

Figure 19. Seismic sparker showing the continuation of the KSfz between MMS profiles 484 and 490. The morphology of this fault scarp shows Holocene sediments draping over in the footwall side of the fault.

ABfz was certainly possible. Previous Holocene earthquakes likely provided motion along this fault system, in any case.

The 1964 Great Alaska Earthquake has megathrust slip partitioned along three separate regions (Ichinose et al., 2007). The PWS asperity led to focused slip along splay faults (Liberty et al., 2013) and a similar tectonic style is observed for the Kodiak asperity. The KSfz is located in the region of 1964 uplift and the zero elevation change isobase separating uplift and subsidence occurs midway on Sitkalidak Island (Figure 20). The greatest interface slip (> 8 m) that Ichinose et al. (2007) calculated (based of 50 km grid cells) can be projected to the KSfz along the nearshore region and encompasses northern Sitkalidak Island. The depth to the megathrust below Sitkalidak Island is approximately 20 km (Hayes et al., 2012) and so splay faults associated with the KSfz

most likely branch directly from the megathrust (or megasplay). My modelled tsunamigenic source locations project to the 6-10 km slip contours at depth along the megathrust, essentially only on cell length from the maximum calculated slip (Figure 20). While my results cannot give constraints on absolute fault uplift, they suggest that 1964 tsunamigenic fault motion resulted in local tsunamis that were sourced very near to the Kodiak Islands shoreline. The impact my results have are to inform tsunami modelers that they should explore the potential of discrete and short fault uplift for tsunami inundation scenarios as a result of megathrust rupture in this region.

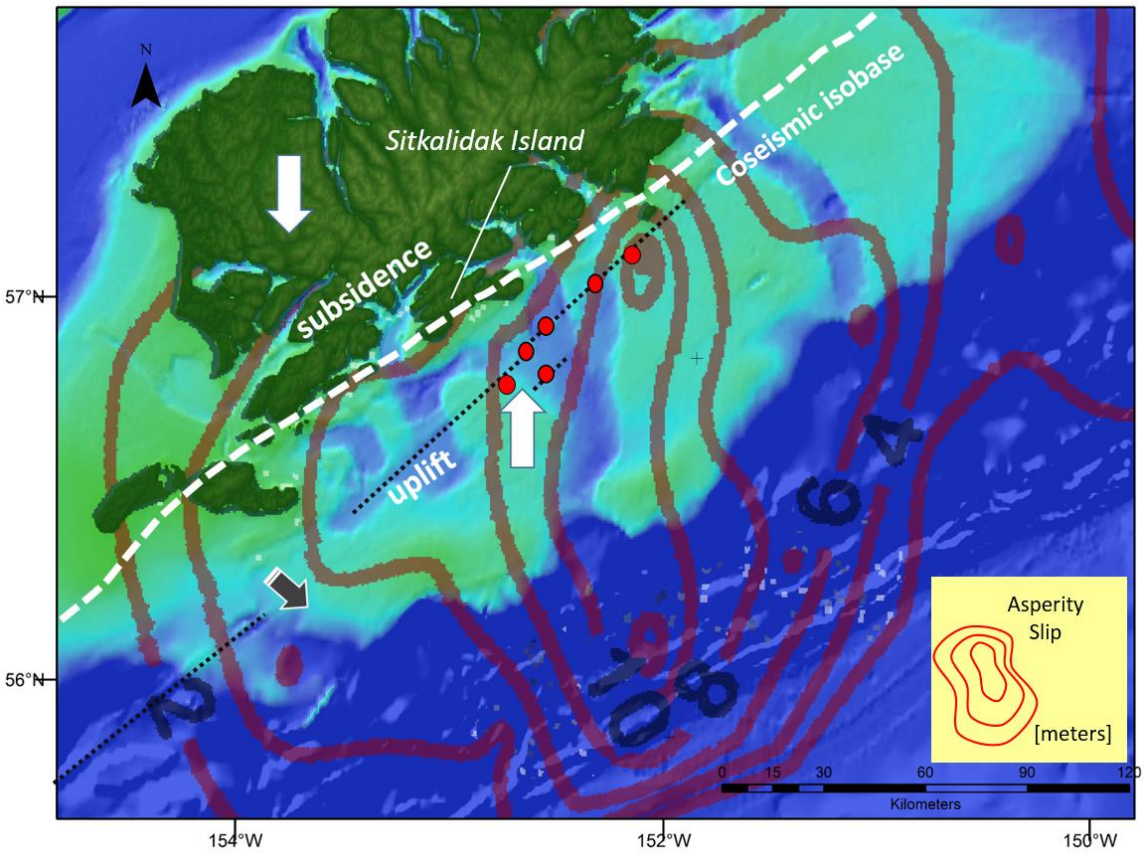

Figure 20. Summary of 1964 tectonic motion. Coseismic subsidence/uplift isobase adapted from (Plafker, 1969). Bold red contours represent asperity slip in meters from the Ichinose et al., (2007) slip model. The small red dots represent locations of prominent fault slip imaged on the MMS seismic lines. The general geometry of the forearc splay faults are to be seaward-stepping, which is emphasized by the dotted

black line and arrow. Note that the modelled tsunamigenic source region is in the location of focused megathrust slip of 8-10 meters from 1964.

CHAPTER FIVE: SOUTHWEST KODIAK SEGMENT BOUNDARY

While Chirikof Island recorded no uplift or subsidence related to the Great Alaska Earthquake of 1964, Sitkinak Island, part of the Trinity Islands, recorded < 1 meter of coseismic uplift, no tsunami wave inundation, and was the southwestern limit of M > 4 aftershocks (Plafker, 1969; Figure 21). Furthermore, the Ichinose et al. (2007) model places the western limit of coseismic slip beneath the Trinity Islands. Figure 21 depicts a summary of 1964 motion, aftershock distribution, uplift and subsidence, and the northern extent of the 1938 M8.2 Semidi rupture (Johnson and Satake, 1994; Briggs et al., 2014). These observations are consistent with the Trinity Islands marking the southwest Kodiak segment boundary.

The quasi-persistent nature of the southwest segment boundary has been inferred from the paleo-earthquake record (Table 1). As evidenced by uplifted shorelines, the AD 1788 event involved joint rupture of the Kodiak and Semidi segments (Briggs et al., 2014). An older megathrust event in AD 1430-1650 involved the Kodiak segment and potentially the Kenai segment, and its rupture boundaries are inferred to lie somewhere along the Kenai Peninsula (Kelsey et al., 2015). The Kodiak segment does not have a robust single or two segment rupture beyond these dates except for the penultimate 1964-type event in AD 1060-1110 which again arrested near Sitkinak (Carver and Plafker, 2008; Kelsey et al., 2015). From these discrete observations, a crude spatiotemporal pattern emerges of alternating single and multi-segment rupture near the southern limits of the Kodiak Islands.

Post-1964 geodetic (presumably interseismic and not post-seismic) measurements suggest the southwest segment megathrust is fully locked between Chirikof and Sitkinak islands (Zweck et al., 2002). The upper plate in this region of the Kodiak segment is therefore coupled to the lower plate and accumulating strain at a rate equal to a plate convergence rate of 62 mm/yr (DeMets et al., 2010). Due to location of measurements on land with respect to subduction zone geometry, the down-dip limit of the locking depth is well-resolved and lies between 30 – 40 km depth to the plate interface, which is beneath the Trinity Islands region and landward of active megathrust splay faults (Zweck et al., 2002; Hayes et al., 2012). A key distinction between the PWS and Kodiak segments is that the highly coupled region below Kodiak is down-dip from a majority of the splay faults that branch out from the megathrust. This is in contrast to PWS where there is greater up-dip locking and permanent shortening of the inner and outer wedge regions (Liberty et al., 2013).

Historic seismicity patterns show that the seaward portion of the southwest Kodiak Islands region has repeatedly had more earthquakes relative to the rest of the segment, which suggests a persistent stress-field across the earthquake cycle in this region (Doser et al., 2002; Doser, 2005; Sauber et al., 2006). Scholz and Campos (2012) showed that megathrust coupling patterns observed during the interseismic period are dependent on the phase of the megathrust earthquake cycle and only in general may asperity and strain accumulation match one another from one earthquake cycle to another. The seismic flux accumulation varies along the megathrust as a function of the earthquake cycle, which is a time-dependent process.

Major structures on the Pacific plate trenchward of the southwest Kodiak Islands include the Aja fracture zone and Patton-Murray seamount chain (Figure 21). Given a Pacific plate convergence direction of N30W, subduction of these sea floor structures generally coincides with the arrest of rupture in 1964 and their combined effect may have been to impede rupture onto the Semidi segment (von Huene et al., 1999; von Huene et al., 2012).

In this chapter, I highlight new gravity and seismic observations and relate them to upper plate structure to further our understanding of splay fault characteristics and seismic hazard. I present evidence to suggest the southwest segment boundary is defined by another subducting fracture zone (Naugler and Wagemen, 1973) and is presently the site of prolific marine terrace erosion and lower crustal underthrusting.

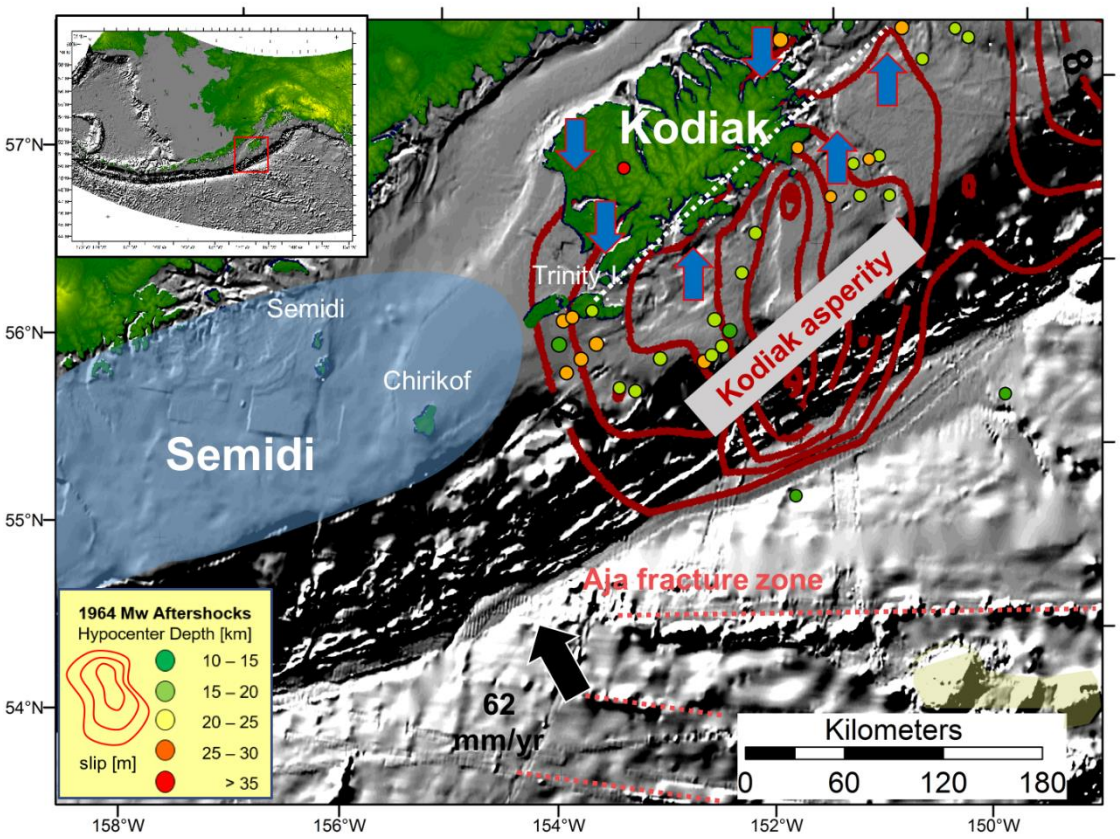

Figure 21. Tectonic summary of 1964 and 1938 motion south of the Kodiak Islands. Approximate location of the Semidi segment is shaded in blue (Carver and Plafker, 2008). Regions of coseismic subsidence and uplift are denoted by blue arrows with the white dashed line marking the 1964 coseismic isobase of zero motion (Plafker, 1969). NDEIC database of aftershocks following the 1964 earthquake are colored by hypocenter depth (see inset legend). 1964 slip is shown as bold, red two-meter contour intervals (Ichinose et al., 2007). Plate convergence rate is from MORVEL plate model (DeMets et al., 2010). Aja fracture zone and seamount chain are highlighted on the Pacific plate. Note that the Trinity Islands mentioned in text refer to both Tugidak and Sitkinak Island. Note the landward step of the continental shelf between Chirikof and Tugidak

Gravity and upper plate structure

I apply a high-pass filter ($\lambda < 70$ km) to the pseudo-Bouguer gravity field to highlight short-wavelength forearc structures (Figure 22). This filter shows a linear, trench-parallel, and positive gravity anomaly across Kodiak (Figure 22 inset). The orientation of this lineament follows the trend of the Kodiak Shelf fault zone (KSfz) and

extends from Kodiak Island southwest to at least Chirikof Island. MMS profiles 514, 516, and 520 cross this lineament at three locations (at 20 and 40 km interval spacing) between the Trinity and Chirikof Islands. These MMS profiles are depth-converted using a 2-D smoothed velocity gradient model and reveal tremendous fault-driven deformation and uplift that are consistent with the gravity signal (Figure 23).

As evidenced by offset strata and a 30 mgal gravity low along MMS 514, I identify two prominent low-angle splay faults that merge below 10 km depth. The landward splay fault shows evidence for folding and back thrusting in the hanging wall that uplifts a keystone style block (Figure 23a). This uplifted region is along strike of the KSfz, contains offset sea floor strata, but did not uplift in 1964. The basin that lies beneath the gravity low region represents the northeastern portion of the Tugidak Basin (Figure 22). The basin is bisected by a thrust and appears to offset strata to the sea floor, and thus may be an active fault. The high-pass filtered and mean-subtracted gravity shows that gravity maxima are consistent with dense hanging wall (Tertiary) strata

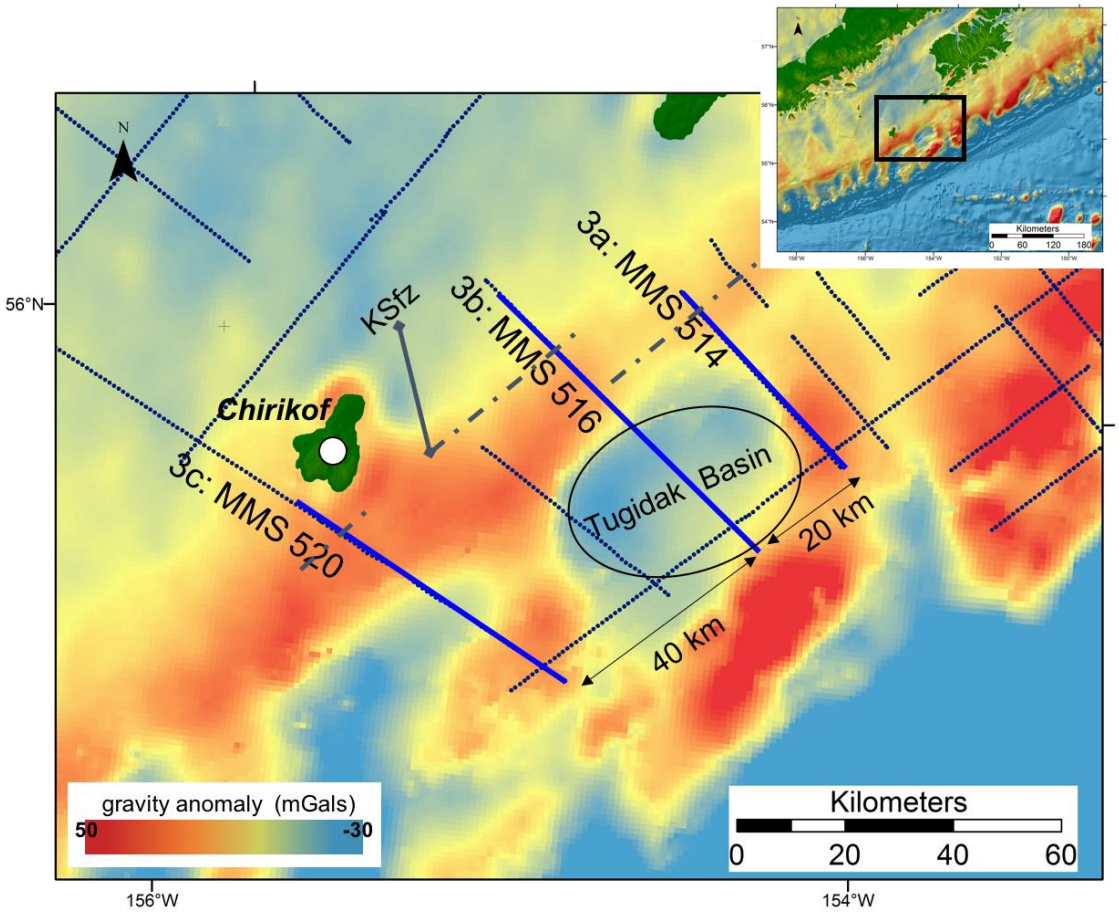

Figure 22. High-pass filtered gravity across the Gulf of Alaska. Inset figure shows larger map location. The MMS profiles discussed in text are highlighted in blue and are labeled according to their order in Figure 23. The Tugidak Basin is interpreted as the negative gravity anomaly. The KSfz is dashed along the MMS profiles that show this feature. Note that MMS line spacing is doubled relative to MMS profiles along the northern Kodiak segment (see Chapters 3 and 4).

a

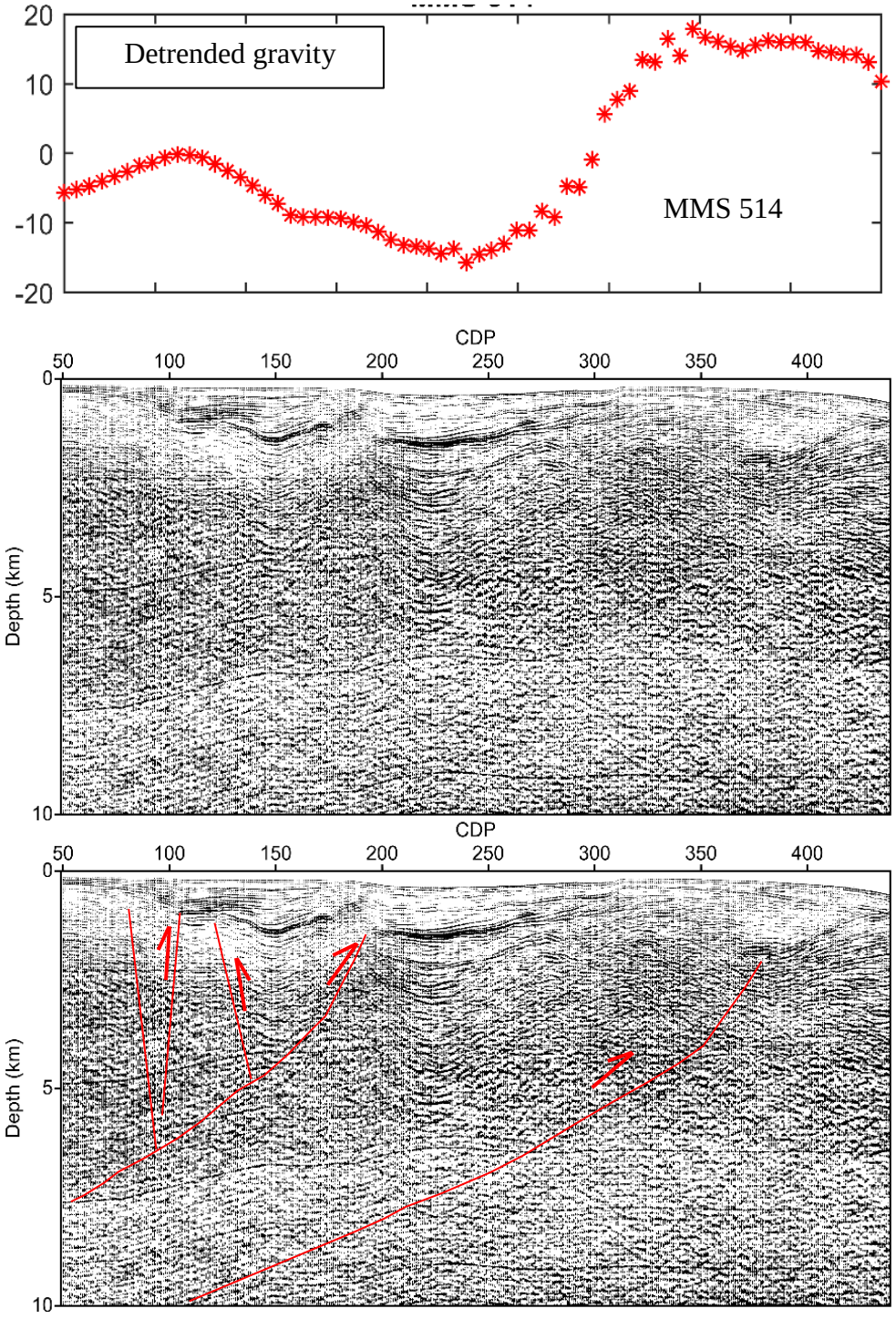
Detrended gravity
MMS 514
20
10
0
-10
-20
CDP
50
100
150
200
250
300
350
400
Depth (km)
0
5
10

b

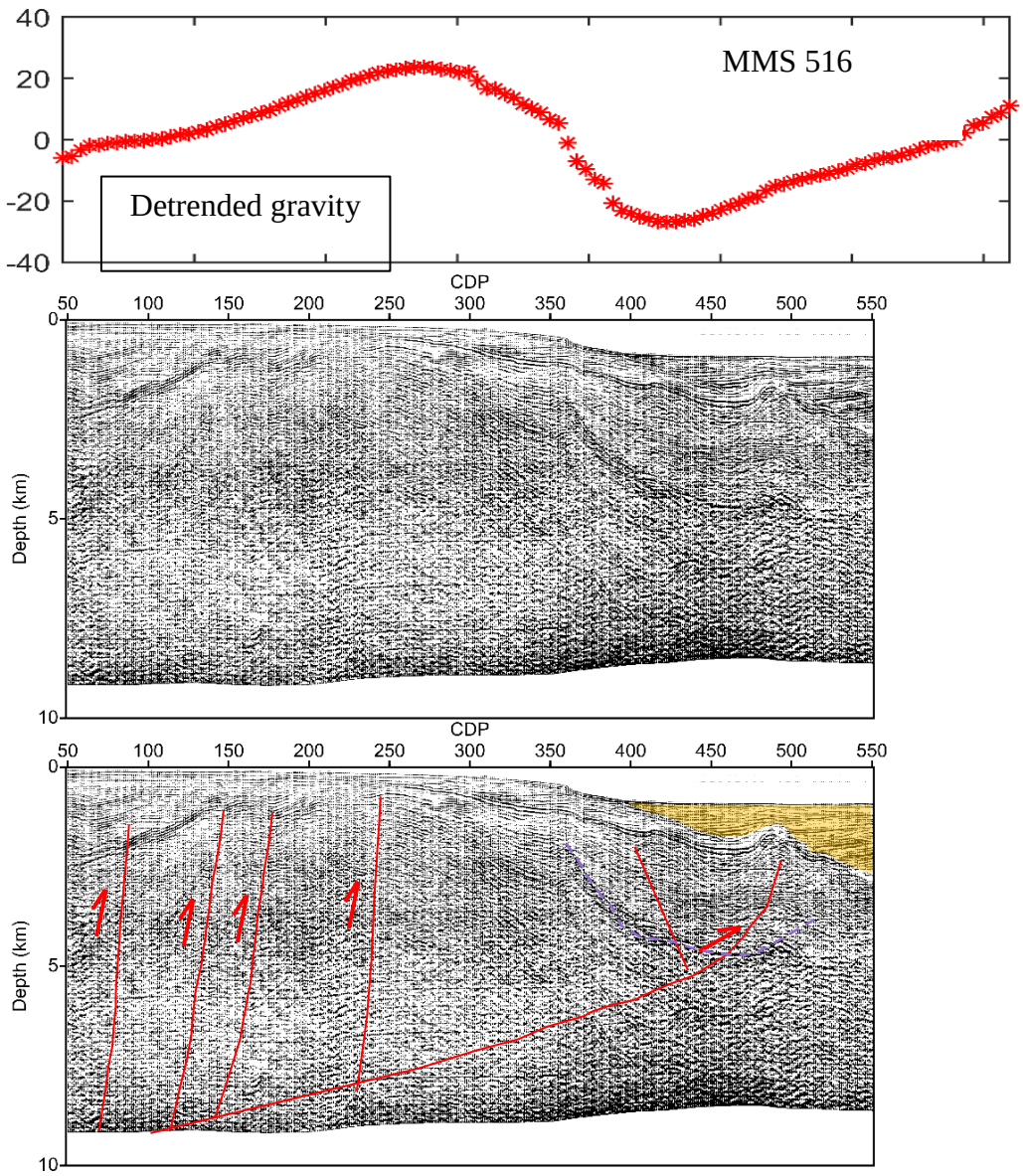

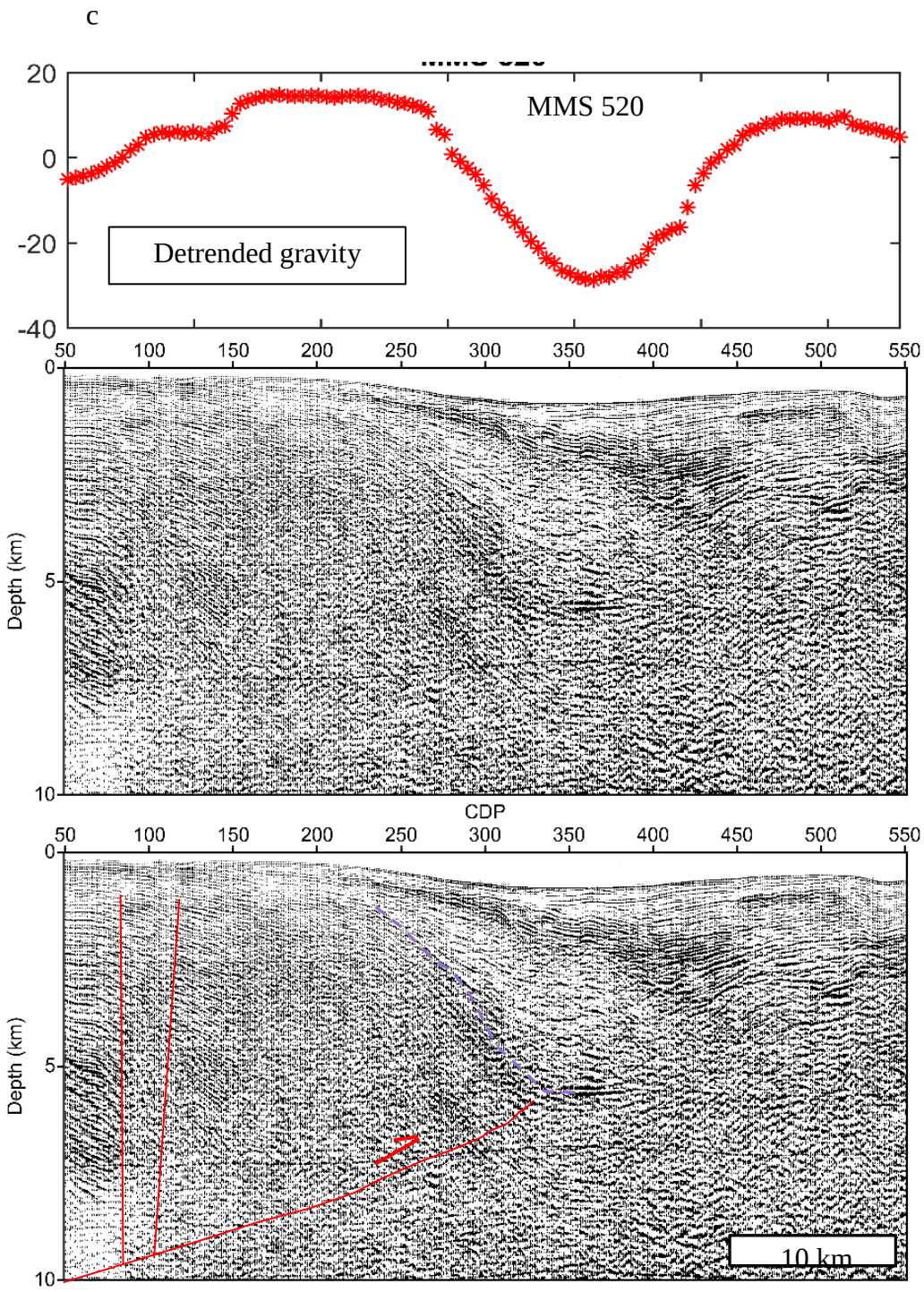

Figure 23. (previous three pages) Depth-converted and interpreted MMS seismic reflection profiles with filtered and mean-subtracted (detrended) pseudo-Bouguer

free-air gravity superposed on top. See Figure 2 for map location. a) MMS line 514 shows two major splay faults and associated structures. b) MMS 516 shows high-angle thrust fault pattern along the first 20 km of the depth-converted profile. Tugidak Basin is shown to be fault controlled. c) MMS 520 marks the last profile of the MMS seismic dataset and images the southernmost extent of the KSfz. On all profiles, positive gravity anomalies are a proxy for Tertiary bedrock exhumation.

juxtaposed with low density (Quaternary) sediments that fill the Tugidak Basin. The southern splay likely uplifts highly deformed strata related to permanent deformation of the accretionary wedge.

MMS 516 crosses the Tugidak Basin (Figure 22) and the basin region is expressed as a 40 mgal gravity low (Figure 23b). The northwest half of MMS 516 shows a relative gravity high and broadly folded strata. The seismic profile images several high-angle thrust faults that fold and offset presumed dense Tertiary and older strata. South-dipping growth strata bound the northern basin margin and bedrock highs beneath the Tugidak Basin appear structurally controlled and bound by a dipping reflector (purple dashed line in 3b). Given the geometry and gravity amplitude, these older strata are likely relic Tugidak Basin sediments. These low angle thrust faults that are typical of accretionary wedge thrusts do not offset Quaternary Tugidak Basin strata and implies they are currently inactive. North dipping strata within the Tugidak Basin imply either a seaward sediment source or fault controlled basin rotation.

MMS 520 seismic profile, located south of Chirikof Island (Figure 22), is characterized by a 20 km wide 20 mgal gravity low that straddles two structural highs (Figure 23c). The northern portion of this profile represents a south-dipping monocline with faults best highlighted by ~5 mgal gravity steps. These faults lie along the KSfz, but clearly lie within the Semidi segment of the subduction zone. The Tugidak basement reflector is again offset and basin folding is related to a low angle thrust.

Two observations that link together these seismic and gravity profiles are the continuity of the KSfz lineament beyond the mapped fault limit and across a major subduction boundary. This analysis shows that gravity and seismic data can map this fault zone and suggests continuation of the KSfz past Chirikof Island (Figure 22). The region between Sitkinak and Chirikof is a semi-persistent segment boundary and a through-going fault zone across this boundary supports and reinforces the potential for uplift of this fault zone when the Semidi and Kodiak segments jointly rupture. Higher quality seismic data may reveal the slip history of this fault system.

The uplift and subsidence record on land argues for both independent and joint rupture of the Kodiak and Semidi segments (Briggs et al., 2014). Independent ruptures of either the ~360 km long Kodiak or ~320 km long Semidi segment support independent M > 8 earthquakes, while joint Kodiak/Semidi ruptures support a M9 event. My results extend the onshore geological evidence of active faulting with Holocene (from an offset sea floor) fault uplift that is associated with the megathrust earthquake cycle near the Kodiak/Semidi segment boundary.

Lower plate and continental shelf structure

The total magnetic field data reveal a conspicuous lineament near the segment boundary between the Trinity and Chirikof Islands (Figure 24). It divides circular magnetic lows within the Semidi and Kodiak segments. This lineament has been previously interpreted as a subducted fracture zone (Naugler and Wageman, 1973; von Huene et al., 2012) and I propose that this fracture zone (hereafter referred to as the Tugidak fracture zone) is controlling upper plate structures and represents an additional constraint on the southwestern limits of the Kodiak asperity. Its projection at depth agrees

well with the limit of resolvable slip from 1964 and also coincides with a 50 km retreat in the continental shelf break (Figure 25).

Assuming the plate boundary geometry is fixed, as represented by the 400 m bathymetric contour, a 50 km landward step in the continental shelf at the segment boundary represents a significant increase in the width of the Kodiak segment deformation front when compared to the adjacent Semidi segment (Figure 25). I measure the deformation front width (D_{fw}) to be the distance between the continental shelf break and the trench axis. Slope profiles oriented normal to the trench across the Kodiak segment show the along-strike variability in the accretionary prism width. Profiles A-A' to C-C' have a D_{fw} of 100, 80, and 80 km, respectively. Profile D-D' crosses the region where the retreat of the shelf break is observed and the D_{fw} widens to approximately 150 km. This suggests that the Kodiak segment continental shelf west of profile D-D’ is currently eroding and excess material is being supplied to the slope and trench (Figure 25). At the cusp of transition in the D_{fw} is the Trinity Basin. The slight structural high that flanks the seaward side of Trinity Basin is a diminishing expression of the continental shelf break (Figure 23b). Active subduction of the Aja fracture zone coupled with a relatively thing subducting sediment volume could provide the mechanical means to assist in this mass-wasting process. A response of the outer wedge of maintain critical taper may then be to increase slope vis-à-vis erosion of the continental shelf break.

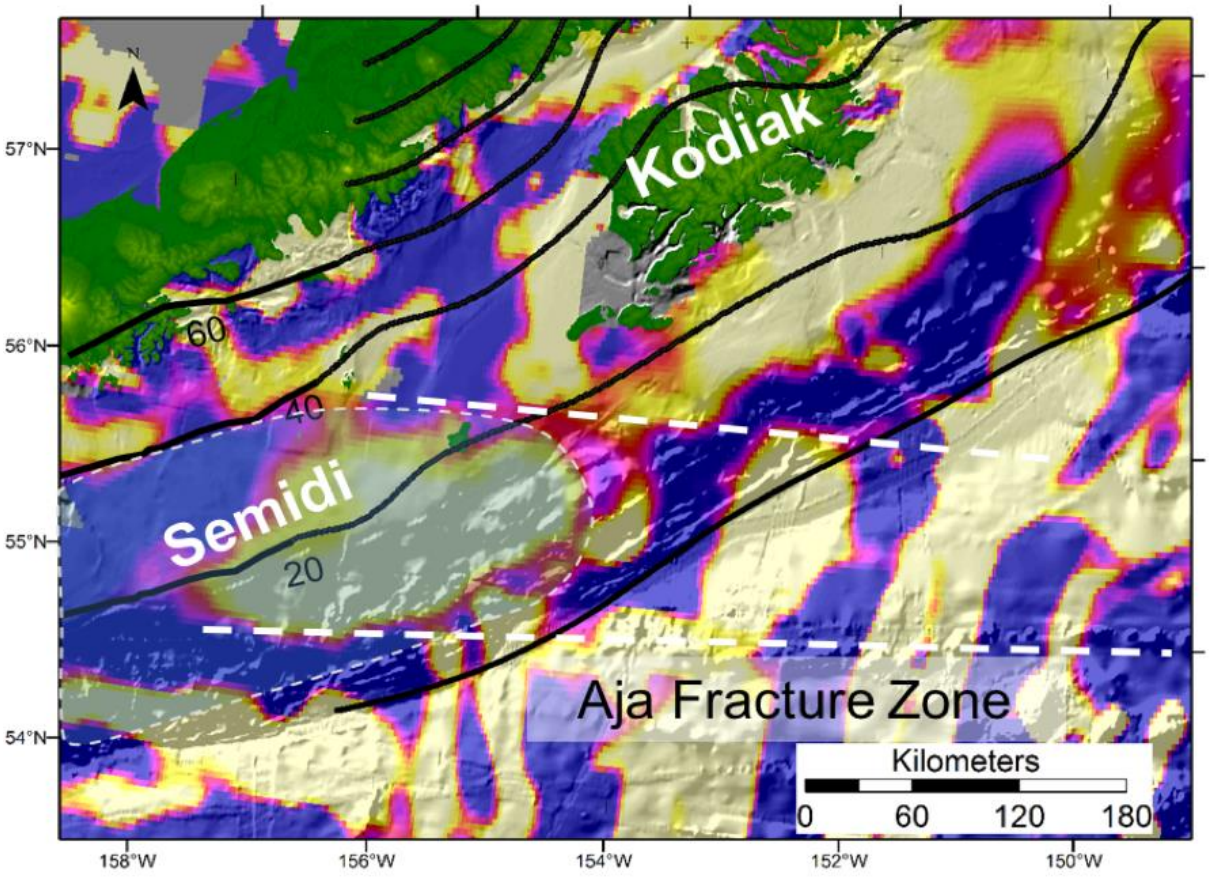

Figure 24. Total field magnetic map across the Kodiak-Semidi region. N85W striking lineation distinguishing a magnetic anomaly high from two magnetic anomaly lows is denoted by the dashed white line (Naugler and Wageman, 1973). This feature coincides with the location of continental shelf retreat. Bold black lines denote depth to plate interface from Slab1.0 (Hayes et al., 2012).

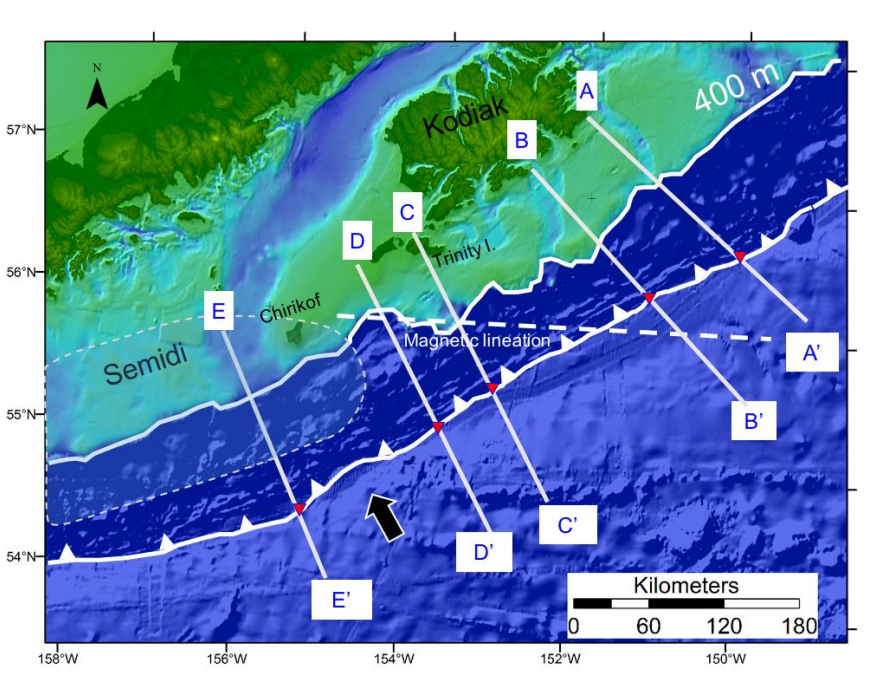
N
57°N
56°N
55°N
54°N
158°W
156°W
154°W
152°W
150°W
Kodiak
400 m
Trinity I.
Chirikof
Semidi
Magnetic lineation
A
A'
B
B'
C
C'
D
D'
E
E'
Kilometers
0 60 120 180

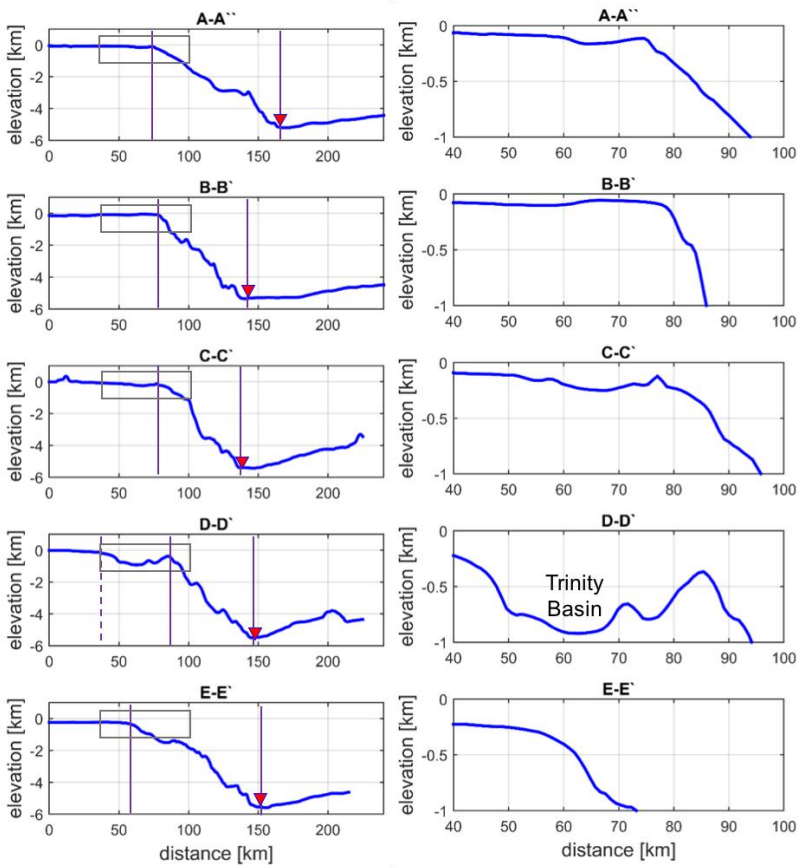
A-A``
B-B`
C-C`
D-D`
E-E`
elevation [km]
distance [km]
Trinity
Basin

Figure 25. (previous page) Physiography of the continental shelf and accretionary prism. Profiles A-A' to E-E' document the changing slope morphology and deformation front width (Dfw). Location of the trench is indicated by the white line with hachured marks (map view) and by the red triangle (cross-sections). The Dfw is denoted by the solid purple lines on each slope cross section. On profile D-D', where the recession of the continental shelf break is observed, the eroding shelf break is the solid purple line and the new shelf break is given by the dashed purple line. The magnetic lineation identified in Figure 24 is superposed to emphasize the coinciding location of margin erosion and subducting structure. Plate convergence direction from MORVEL plate model (DeMets et al., 2010).

Interseismic observations

The southwest portion of the Kodiak segment experiences greater interseismic moment-release relative to the rest of the Kodiak segment (Doser et al., 2002). In particular, focal mechanisms indicative of low-angle, lower crustal thrusting dominate the interseismic character of intermediate ($5 < Mw < 7$) magnitude events in this region (Figure 26). The population of low-angle thrust earthquakes are also unique in the respect that this density and focal mechanism type does not continue beneath the Semidi segment. Calculated seismic flux shows a region of focused energy-release that, according to the Slab1.0 plate model (Hayes et al., 2012) is occurring within the subducting Pacific plate (Figures 26 and 27). The North American plate at an interface depth of 20 km is strongly coupled to the Pacific plate, and yet the majority larger events are occurring up-dip of this region (Zweck et al., 2002). Plate locking estimates from GPS geodesy suggests the greatest accumulated strain lie at depth between Chirikof and the Trinity Islands (Figure 26). I project several focal mechanisms to a profile near the Kodiak/Semidi segment boundary to show that common fault planes could be the interseismic expression of underthrust lithospheric material (Figure 27).

The Gulf of Alaska convergent margin is considered to be an accretionary margin at the regional level. Locally, however, there exists a cyclic behavior to the processes of

outer wedge accretion and deformation (Gutscher et al., 1998). A steep slope angle does not allow the outer wedge to sustain great overburden stresses and as a result, the outer wedge responds by imbricate thrusting near the trench; a companion process involves the underthrusting of long, un-deformed sheets when the slope angle is shallower (Gutscher et al., 1996, 1998).

The observations of retreating continental slope break (growing deformation front width) and dominant low-angle thrust focal mechanisms suggest the southwest Kodiak segment boundary is switching to the frontal accretion phase of the accretionary cycle. This transition appears to occur over approximately 200 km of the Kodiak segment. The focal mechanisms at depth may be indicative of long, thrust sheet structures (~100 km length), so the underthrusting phase is still persistent, but an eroding slope will to decrease slope angle and return the margin to accretion.

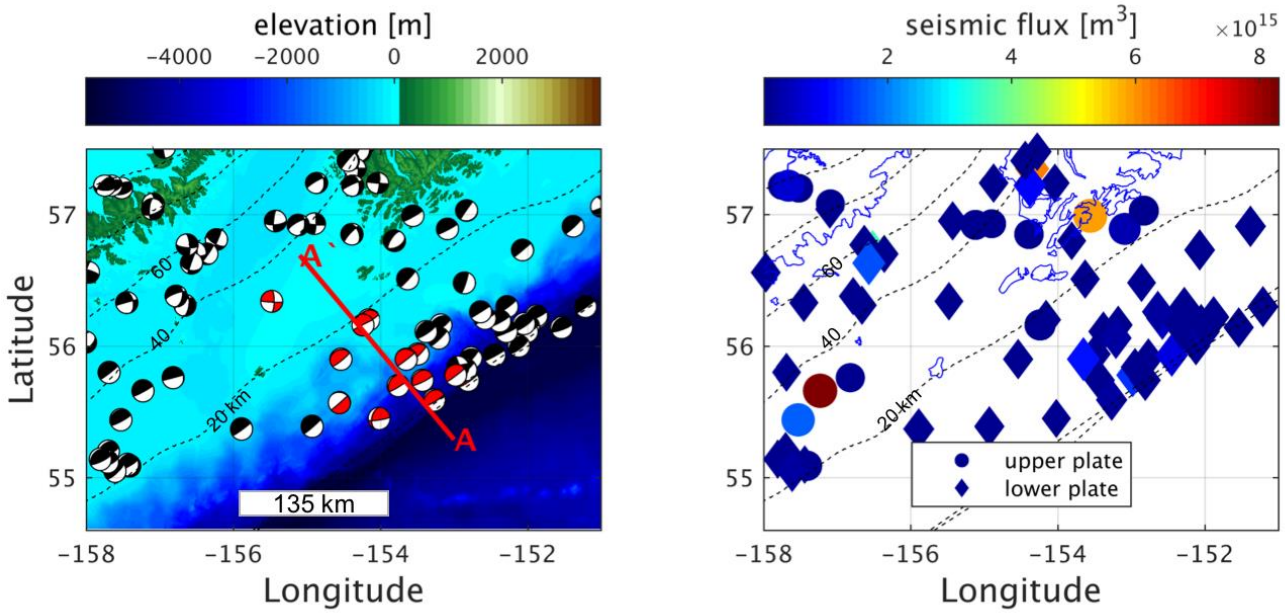

Figure 26. Focal mechanisms across the Kodiak/Semidi boundary. Left figure shows the distribution of focal mechanisms overlain on top of the Gulf of Alaska DEM (Lim et al., 2011). A cross section labeled A-A' in red is explored in Figure 27. Right figure is the calculated seismic flux for all focal mechanism events (see Methods for discussion of seismic flux). Diamonds denote lower plate events and circles are upper plate events (relative to Slab1.0 model). On both plots, interface depth is given by dashed black marks in contours of 20 km. Focal mechanisms are from the Harvard CMT database (Dziewonski et al., 1981; Ekstrom et al., 2012).

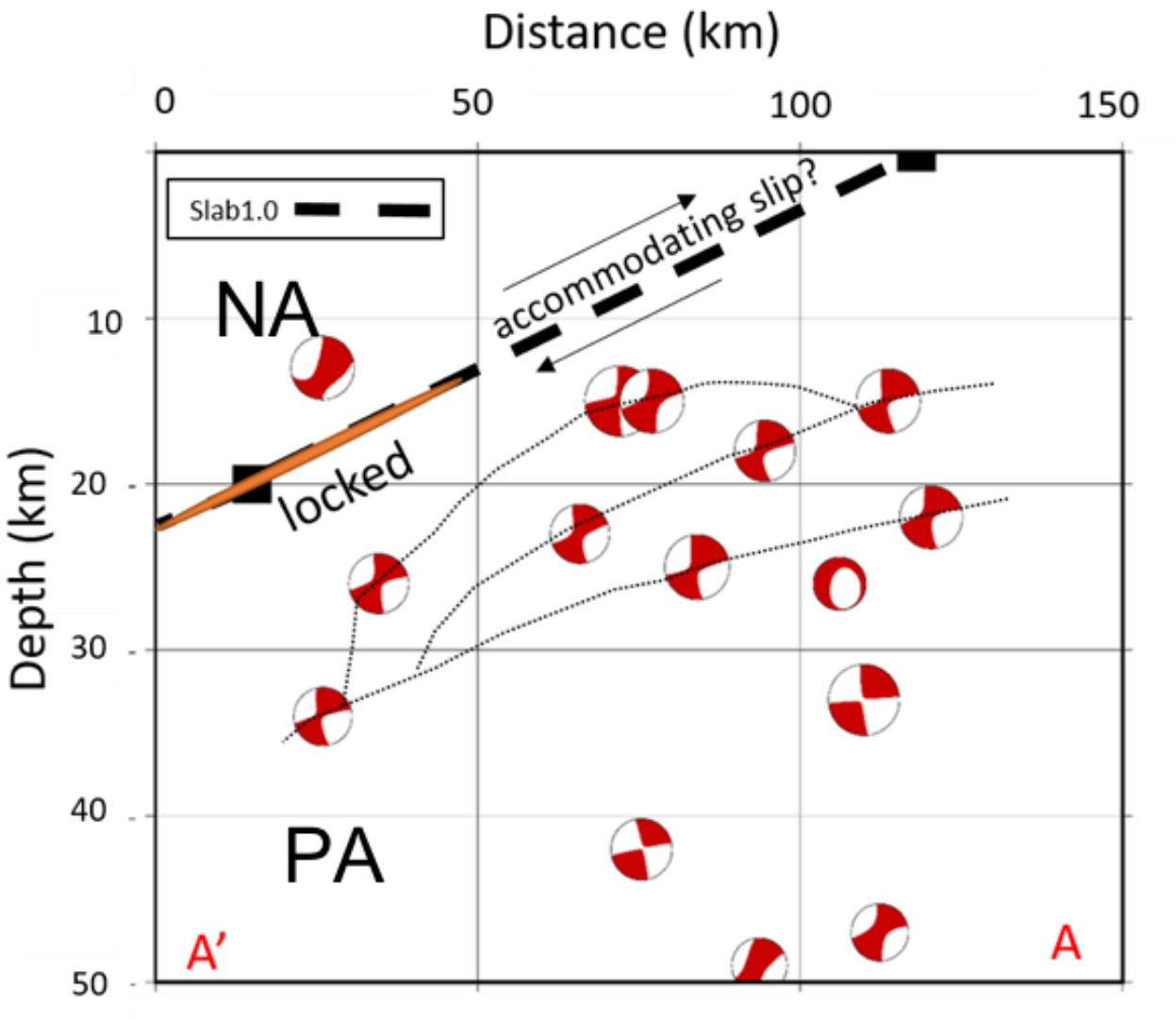

Figure 27. ossible seismotectonic interpretation across profile A-A' (see figure 26 for location). Focal mechanisms are projected with interpreted fault planes at depth. Slab1.0 plate model is appended for comparison. The locked region of megathrust is highlighted in orange according to the Zweck et al., (2002) coupling model. NA and PA stand for North American and Pacific plates, respectively.

Persistence of the southwest segment boundary

The southwest Kodiak/Semidi segment boundary is defined by several unique geophysical and structural characteristics. There is the interpreted Tugidak fracture zone subducting at a N85W trending strike that coincides with significant erosion of the continental slope and a clustering of shallow, low-angle thrust focal mechanisms. This suggests a relationship between erosion, subducting topography, and the rupture limit of both the 1938 Semidi and 1964 Great Alaska Earthquake megathrust events. Gravity and upper crustal scale seismic reflection data show the continuation of the KSfz through the southwest segment boundary on the upper plate and this agrees with models for joint rupture of the Kodiak and Semidi boundary, though this portion of the KSfz did not rupture in 1964.

CHAPTER SIX: CONLCUSIONS

The Kodiak Islands region has a complex spatiotemporal history of megathrust rupture. Different paleoseismic models have tried to reconstruct this history and assess general segment boundaries across Kodiak (e.g. Shennen et al., 2007; Carver and Plafker, 2008; Briggs et al., 2014; Shennan et al., 2014; Kelsey et al., 2015). Modern geophysical investigations have characterized asperity distribution, megathrust geometry, and post-1964 deformation for the 1964 Great Alaska Earthquake (Brocher et al., 1994; Doser et al., 2002; Zweck et al., 2002; Eberhardt-Phillips et al., 2006; Li et al., 2013). But these studies have not reconciled geophysical observations in conjunction with upper plate structure or proffered a comprehensive kinematic model for how subducting structure on the incoming Pacific plate may be influencing upper plate deformation and vice-versa.

I have analyzed various datasets to make the first step towards a composite tectonic picture of how the Kodiak Islands region fits into the megathrust earthquake cycle in the Gulf of Alaska. Northeast Kodiak is defined by the subducting 58° fracture zone and this feature has been related to changing seismotectonic conditions across the upper and lower plates relative to the rest of the Kodiak segment. During great earthquakes (M~9) that involve the PWS segment this fracture zone most likely does not impede rupture (i.e. 1964), but potentially could for single segment type earthquakes.

I have shown a link between margin erosion and lower plate seismicity in the southwest Kodiak segment where the 1964 Great Alaska earthquake rupture ceased.

Additionally, there is a possible structural control of the Tugidak fracture zone on the arrest of the 1964 Great Alaska Earthquake.

Both fracture zones and seamounts are common Pacific plate morphologies and their subduction most likely influences the megathrust earthquake cycle by filling in the rupture gap between great earthquakes. As the paleoseismic record attests to, the Kodiak segment participates in both single and multi-segment rupture and segment boundaries that encompass successive megathrust earthquake cycles may not exist for this region. It is more appropriate to allow for a variety of megathrust rupture scenarios across this segment and there is geophysical evidence to place segment boundaries between the 58° and Tugidak fracture zones. The novelty of this thesis is in relating subducting lower plate topography to observations of interseismic deformation and upper plate structure.

Tsunami travel-time modelling that I conducted offers an updated view on how tsunamigenic faults uplift in response to megathrust slip offshore of the Kodiak Islands. The exceptional spatial variability in the KSfz seafloor scarp height emphasizes discrete and short (< 30 km) uplift patterns that may have persisted through the Holocene epoch. My results suggest a clear need to include these kinds of short rupture scenarios in current tsunami inundation modelling and capture the near-shore risk to Kodiak Island residents.

REFERENCES

Ammon, C. J., Lay, T., Kanamori, H., and Cleveland, M. (2011), A rupture model of the 2011 off the Pacific coast of Tohoku Earthquake, *Earth, Plan., Space*, 63. 7. 693-696.

Bassett, D., and A. B. Watts (2015a), Gravity anomalies, crustal structure, and seismicity at subduction zones: 1. Seafloor roughness and subducting relief, *Geochem. Geophys. Geosyst*., 16, 1508–1540, doi:10.1002/ 2014GC005684.

Bassett, D., and A. B. Watts (2015b), Gravity anomalies, crustal structure, and seismicity at subduction zones: 2. Interrelationships between fore-arc structure and seismogenic behavior, *Geochem. Geophys. Geosyst*., 16, 1541– 1576, doi:10.1002/2014GC005685.

Blakely, R. J., Brocher, T. M., and Wells, R. E. (2005), Subduction zone magnetic anomalies and implications for hydrated forearc mantle, *Geology*, 33 (6), 445-448, doi: 10.1130/G21447.1.

Blakely, R. J. (1996), Potential Theory in Gravity and Magnetic Applications, Cambridge University Press, Cambridge, United Kingdom, 441 pages.

Bilek, S.L., Schwartz, S. Y., and DeShon, H. R. (2003), Control of seafloor roughness on earthquake rupture behavior, *Geology*, 31, 5, 455-458.

Briggs, R.W., S. E. Engelhart, A. R. Nelson, T. Dura, A.C. Kemp, P. J. Haeussler, D. R. Corbett, S. J. Angster, and L.-A. Bradley (2014), Uplift and subsidence reveal a nonpersistent megathrust rupture boundary (Sitkinak Island, Alaska), *Geophys. Res. Lett.*, 41, 2289–2296.

Brocher, T. M., G. S. Fuis, M. A. Fisher, G. Plafker, M. J. Moses, J. J. Taber, and N. I. Christensen (1994). Mapping the megathrust beneath the northern Gulf of Alaska using wide-angle seismic data, *J. Geophys. Res*. 99, 11,663–11,686.

Brothers, D. S., Haeussler, P. J., Liberty, L. M., Finlayson, D., Geist, E., Labay, K., and Byerly, M. (2016), A submarine landslide source for the devastating 1964 Chenega tsunami, southern Alaska, *Earth & Planet. Sci. Lett.*, 438, 112-121.

Carver, G., Sauber, J., Lettis, W., Witter, R., and Whitney, B. (2008), Active faults on Northeastern Kodiak Island, Alaska, in *Active Tectonics and Seismic Potential of Alaska, Geophys. Monogr. Ser.*, vol. 179, edited by J. T. Freymueller et al., pp. 167-184, AGU, Washington, D. C.

Carver, G. and Plafker, G. (2008), Paleoseismicity and neotectonics of the aleutian subduction zone—An overview, in *Active Tectonics and Seismic Potential of Alaska, Geophys. Monogr. Ser.*, 179, edited by J. T. Freymueller et al., 43–63, AGU, Washington, D. C.

Clendenen, W. S., Sliter, W. V., Bryne, T. (1990), Tectonic implications of the Albatross sedimentary sequence, Sitkinak Island, Alaska, *U.S. Geol. Surv.*, 52-70.

Cloos, M. (1992), Thrust-type subduction-zone earthquakes and seamount asperities: A physical model for seismic rupture, *Geology*, 20, 601–604.

DeMets, C., Gordon, R. G., and Argus, D. F. (2010), Geologically current plate motions, *Geophys. J. Int.*, 181, 1-80.

Doser, D., Brown, W. A., and Velasquez, M. (2002), Seismicity of the Kodiak Island region (1964-2001) and its relation to the 1964 Great Alaska Earthquake, *Bull. Seismol. Soc. Am.*, 92, 3269-3292.

Doser, D. (2005), Historical Seismicity (1918-1964) of the Kodiak Island Region, *Bull. Seismol. Soc. Am.*, 95, 878-895.

Doser, D. (2006), Relocations of Earthquakes (1899-1917) in South-Central Alaska, *Pure and App. Geophys.*, 163, 1416-1476.

Dragert, H., Hyndman, R.D., Rogers, G.C., and Wang, K. (1994), Current deformation and the width of the northern Cascadia subduction thrust, *J. Geophys. Res.*, 99, 653-668.

Dziewonski, A. M., T.-A. Chou and J. H. Woodhouse, Determination of earthquake source parameters from waveform data for studies of global and regional seismicity, *J. Geophys. Res.*, 86, 2825-2852, 1981. doi:10.1029/JB086iB04p02825

Eberhart-Phillips, D., D. H. Christensen, T. M. Brocher, R. Hansen, N. A. Ruppert, P. J. Haeussler, and G. A. Abers (2006), Imaging the transition from Aleutian subduction to Yakutat collision in central Alaska, with local earthquakes and active source data, *J. Geophys. Res*., 111, B11303, doi:10.1029/2005JB004240.

Ekström, G., M. Nettles, and A. M. Dziewonski (2012), The global CMT project 2004-2010: Centroid-moment tensors for 13,017 earthquakes, *Phys. Earth Planet. Inter*., 200-201, 1-9, doi:10.1016/j.pepi.2012.04.002

Fisher, M. A., and von Huene, R. (1980), Structure of the upper Cenozoic strata beneath Kodiak shelf, Alaska, *AAPG Bull*., 64, 1014–1033.

Fisher, D., and Byrne, T. (1987), Structural evolution of underthrusted sediments, Kodiak Islands, Alaska, *Tectonics*, 6, 775–793.

Fournier, T. J., and J. T. Freymueller (2007), Transition from locked to creeping subduction in the Shumagin region, Alaska, *Geophys. Res. Lett*., 34, L06303, doi:10.1029/2006GL029073.

Fruehn, J., von Huene, R., and Fisher, M. (1999), Accretion in the wake of terrane collision: The Neogene accretionary wedge off Kenai Peninsula, Alaska, *Tectonics*, 18, 263-277.

Gulick, S. P. S., Jaeger, J. M., Mix, A. C., Asahi, H., Bahlburg, H., Belanger, C. L., Swartz, J. M. (2015), Mid-Pleistocene climate transition drives net mass loss from rapidly uplifting St. Elias Mountains, Alaska. *Proceedings of the National Academy of Sciences*, 1–6. http://doi.org/10.1073/pnas.1512549112

Gutscher, M. A., Kukowski, N., Malavielle, J., and Lallemand, S. (1996), Cyclical behavior in thrust wedges: Insights from high basal friction sandbox experiments, *Geology*, 24, 135-138.

Gutscher, M. A., Kukowski, N., Malavielle, J., and Lallemand, S. (1998), Episodic imbricate thrusting and underthrusting: Analog experiences and mechanical analysis applied to the Alaska Accretionary Wedge, *J. Geophys. Res.*, 103, p 10,161-176.

Gutscher, M. A., and S. M. Peacock (2003), Thermal models of flat subduction and the rupture zone of great subduction earthquakes, *J. Geophys. Res.*, 108(B1), doi:10.1029/2001JB000787.

Haeussler, P. J., Bradley, D. C., Wells, R. E., and Miller, M. L. (2003), Life and death of the Resurrection plate: evidence for its existence and subduction in the northeastern Pacific in Paleocene-Eocene time, *GSA Bull.*, 115, 867-880.

Haeussler, P. J., Armstrong, P. A., Liberty, L. M., Ferguson, K. M., Finn, S. P., Arkle, J. C., and Pratt, T. L. (2015) Focused exhumation along megathrust splay faults in Prince William Sound, Alaska, *Quat. Sci. Rev.*, 113, 8-22.

Hayes, G. P., D. J. Wald, and R. L. Johnson (2012), Slab1.0: A three-dimensional model of global subduction zone geometries, *J. Geophys. Res*., 117, B01302, doi:10.1029/2011JB008524.

Heuret, A., Conrad, C.P., Funiciello, F., Lallemand, S., and Sandri, L. (2012), Relation between subduction megathrust earthquakes, trench sediment thickness, and upper plate strain, *Geophys. Res. Lett.*, 39, L05304, doi:10.1029/2011GL0507012.

Hutchinson, I. and Crowell, A. (2007), Recurrence and extent of great earthquakes in southern alaska during the late Holocene from an analysis of the radiocarbon record of land-level change and village abandonment, *Radiocarbon*, 49, 3, 1323-1385.

Ichinose, G., P. Somerville, H. K. Thio, R. Graves, and D. O'Connell (2007), Rupture process of the 1964 Prince William Sound, Alaska, earthquake from the combined inversion of seismic, tsunami, and geodetic data, *J. Geophys. Res*., 112, doi:10.1029/2006JB004728.

Johnson, J. M. and Satake, K. (1994), Rupture extent of the 1938 Alaskan earthquake as inferred from tsunami waveforms, *Geophys. Res. Lett*., 21, 733-736.

Johnson, J. M., Satake, K., Holdahl, S. R., and Sauber, J. (1996) The 1964 Prince William Sound earthquake: joing inversion of tsunami and geodetic data, *J. Geophys. Res.*, 101(B1), 523-532.

Kaufman, D. S., and W. F. Manley (2004), Pleistocene maximum and Late Wisconsin glacier extents across Alaska, U.S.A., in *Quaternary Glaciations—Extent and Chronology, Part II: North America. Developments in Quaternary Science*, vol. 2, edited by J. Ehlers, and P. L. Gibbard, pp. 9–27, Elsevier, Amsterdam.

Kelsey, H.M., R.C. Witter, S.E. Engelhart, R. Briggs, A., Nelson, P. Haeussler, and D.R. Corbett (2015), Beach ridges as paleoseismic indicators of abrupt coast subsidence during subduction zone earthquakes, and implications for Alaska-Aleutian subduction zone paleoseismology, southeast coast of the Kenai Peninsula, Alaska, *Quat. Science Rev.*, 113, 147-158.

Kennet, J. P. (1982), Marine Geology, Prentice Hall, New Jersey, United States, 813 pages.

Kim, Y., G. A. Abers, J. Li, D. Christensen, J. Calkins, and S. Rondenay (2014), Alaska Megathrust 2: Imaging the megathrust zone and Yakutat/Pacific plate interface in the Alaska subduction zone, *J. Geophys. Res.*:*Solid Earth*, 119, 1924–1941, doi:10.1002/2013JB010581

Lay, T., H. Kanamori, and L. J. Ruff (1982), The asperity model and the nature of large subduction zone earthquakes, *Earthquake Predict. Res.*, 1, 3–71.

Lebrun, J. F., Karner, G. D., and Collot, J. Y. (1998), Fracture zone subduction and reactivation across the Puysegur ridge/trench system, southern New Zealand, *J. Geophys. Res.*, 103, 7293-7313.

Li, J., G. A. Abers, Y. H. Kim, and D. Christensen (2013), Alaska megathrust 1: Seismicity 43 years after the great 1964 Alaska megathrust earthquake, *J. Geophys. Res.: Solid Earth*, 118, 4861–4871, doi:10.1002/jgrb.50358.

Liberty, L. M., Finn, S. P., Haeussler, P. J., Pratt, T. L., and Peterson, A. (2013), Megathrust splay faults at the focus of the Prince William Sound asperity, Alaska,

J. Geophys. Res.: Solid Earth, *118*(10), 5428–5441. http://doi.org/10.1002/jgrb.50372.

Lim, E., B.W. Eakins, and R. Wigley, Coastal Relief Model of Southern Alaska: Procedures, Data Sources and Analysis, NOAA Technical Memorandum NESDIS NGDC-43, 22 pp., August 2011.

Lowrie, W. (2007), Fundamentals of Geophysics, Cambridge University Press, Cambridge, UK, 381 pages.

Lu, Z. and Wyss, M. (1996), Segmentation of the Aleutian plate boundary derived from stress direction estimates based on fault plane solutions, *J. Geophys. Res*, 101, 803-816.

Manard, H. W. and Atwater, T. (1969), Origin of fracture zone topography, *Nature*, 1037-1040.

Maus, Steven (2009), EMAG2: Earth Magnetic Anomaly Grid (2-arc-minute resolution). National Geophysical Data Center, NOAA. Model. doi:10.7289/V5MW2F2P [May 2016].

Moore, J. C. and Allwardt, A. (1980), Progressive deformation of the Tertiary trench slope, Kodiak Islands, Alaska, *J. Geophys. Res.*, 85, 4741-4756.

Moore, J. C., Bryne, T., Plumely, P. W., Reid, M., Gibbons, H., and Coe, R. S. (1983), Paleogene evolution of the Kodiak Islands, Alaska: Consequences of ridge-trench interaction in a more southerly latitude, *Tectonics*, 2, 265-293.

Moore, J. C., Diebold, J., Fisher, M. A., Sample, J., Brocher, T., Talwani, M., Ewing, J., von Huene, R., Rowe, C., Stone, D., Stevens, C., and Sawyer, D. (1991), EDGE deep seismic reflection transect of the eastern Aleutian arc-trench layered lower crust reveals underplating and continental growth, *Geology*, 19, 420-424.

Naugler, F. P. and Wageman, J. M. (1973), Gulf of Alaska: Magnetic Anomalies, Fracture Zones, and Plate Interaction, *GSSA Bull.*, 84, 1575-1584.

Plafker, G. (1969), Tectonics of the March 17, 1964 Alaska earthquake, *U.S. Geol. Surv. Prof. Pap.*, 543-I, 74.

Plafker, G. (1972), The Alaskan earthquake of 1964 and Chilean earthquake of 1960: Implications for arc tectonics and tsunami generation, *J. Geophys. Res.*, 77(5), 901-925.

Plafker, G., Moore, J. C., and Winkler, G. R. (1994), Geology of the southern Alaska margin, *in* Plafker, G., Moore, and Berg, H. C., eds., The Geology of Alaska: Boulder, Colorado, Geological Society of America, The Geology of North America, v G-1.

Porto, N. M. and Fitzenz, D. D. (2016), An alternative segmentation model for the Alaska Aleutian megathrust, *BSSA.*, 106, 3, 1125-1132.

Ratchkovski, N. A. and Hansen, R. A. (2001), Sequence of strong intraplate earthquakes in the Kodiak Island region, Alaska in 1999-2001, *Geophys. Res. Lett.*, 28, 19, 3729-3932.

Reece, R.S., Gulick, S.P.S., Horton, B.K., Christeson, G.L., and Worthington, L.L. (2011), Tectonic and climatic influence on the evolution of the Surveyor fan and channel system, Gulf of Alaska, *Geosphere*, 7, 4, 830–844, doi: 10.1130/GES00654.1.

Robinson, D. P. and Watts, A. B. (2006), Earthquake rupture stalled by a subducting fracture zone, *Science*, 312, 1203-1205.

Ruff, L. and Kanamori, H. (1983), Seismic coupling and uncoupling at subduction zones, *Tectonophysics*, 99, 99-117.

Ryan, H. F., von Huene, R., Wells, R. E., Scholl, D. W., Kirby, S., and Draut, A. E. (2011), History of Earthquakes and Tsunamis along the Eastern Alaska-Aleutian Megathrust, with implications for tsunami hazards in the California continental borderland, *U.S. Geol. Surv. Prof. Pap.*, 1795-A, 2.

Sandwell, D. T. (1984), Thermomechanical evolution of oceanic fracture zones, *J. Geophys. Res.*, 89 (B13), 11401-1113

Sandwell, D. T., R. D. Müller, W. H. F. Smith, E. Garcia, R. Francis (2014), New global marine gravity model from CryoSat-2 and Jason-1 reveals buried tectonic structure, *Science*, 346 (6205), 65-67, doi: 10.1126/science.1258213.

Saltus, R.W., Hudson, T.L., and Wilson, F.H. (2007), The geophysical character of southern Alaska—Implications for crustal evolution, in Ridgway, K.D., Trop, J.M., Glen, J.M.G., and O'Neill, J.M., eds., Tectonic Growth of a Collisional Continental Margin: Crustal Evolution of Southern Alaska: Geological Society of America Special Paper 431, p. 1–20, doi: 10.1130/2007.2431(01).

Sauber, J., G. Carver, S. Cohen, and R. King (2006), Crustal deformation and the seismic cycle across the Kodiak Islands, Alaska, *J. Geophys. Res*., 111, B02403, doi:10.1029/2005JB003626.

Scholz, C. H., and J. Campos (2012), The seismic coupling of subduction zones revisited, *J. Geophys. Res*., 117, B05310.

Shennan, I., Bruhn, R., and Plafker, G. (2009), Multi- segment earthquakes and tsunami potential of the Aleutian megathrust, *Quat. Sci. Rev*., 28, 7–13, doi: 10 .1016 /j .quascirev .2008.09.016.

Shennan, I., N. Barlow, G. Carver, F. Davies, E. Garrett, and E. Hocking (2014), Great tsunamigenic earthquakes during the past 1000 yr on the Alaska megathrust, *Geology*, 42, 687-690.

Shillington, D.J.; Bécel, A., Nedimović, M.R., Kuehn, H., Webb, S.C. Abers, G.A., Keranen, K.M.; Li, J.; Delecluse, M.; Mattei-Salicrup, G.A. (2015), Link between plate fabric, hydration and subduction zone seismicity in Alaska, *Nature Geosci.*, 8, 961-964, doi:10.1038/ngeo02586

Smith, W. H. F. and Sandwell, D. T. (1997), Global seafloor topography from satellite altimetry and ship depth soundings, *Science*, 277, 1957-1962.

Song, T. A. and Simons, M. (2003) Large trench-parallel gravity variations predict seismogenic behavior in subduction zones, *Science*, 301, 630-632.

Stern, R. J. (2002), Subduction Zones, *Rev. Geophys.*, 40(4), 1012, doi:10.1029/2001RG000108.

Stevenson, A.J., and Embley, R. (1987), Deep sea fan bodies, terrigenous turbidite sedimentation, and petroleum geology, Gulf of Alaska, in Scholl, D.W., et al., eds., Geology and resource potential of the continental margin of western North America and adjacent ocean basins—Beaufort Sea to Baja California: Circum-Pacific Council for Energy and Mineral Resources, *Earth Science Series*, 6, 503–522.

Suito, H., and J. T. Freymueller (2009), A viscoelastic and afterslip postseismic deformation model for the 1964 Alaska earthquake, *J. Geophys. Res*, doi:10.1029/2008JB005954.

Suleimani, E. N., Hansen, R. A., and Kowalik, Z. (2003), Inundation modeling of the 1964 tsunami in Kodiak Island, Alaska, *Submarine Landslides and Tsunamis*, 191-202.

Turner, R. F. (1987), Geological and operational summary, Kodiak Shelf stratigraphic test wells, Western Gulf of Alaska, In R. F. Turner ed., Geological and operational summary, Kodiak Shelf Stratigraphic Test Wells, Alaska, Minerals Management Service OCS Report MMS 87-0109.

von Huene, R., M. A. Hampton, M. A. Fisher, D. J. Varchol, and G. R. Cochrane (1980), Near-surface geologic structures, Kodiak Shelf, Alaska. 1:500,000, Map MF-1200, U.S. Geol. Survey, Misc. Field Stud.

von Huene, R., Fisher, M. A., and Bruns, T. R. (1987), Geology and evolution of the Kodiak margin, Gulf of Alaska, in Geology and Resource Potential of the Continental Margin of Western North America and Adjacent Ocean Basins-Beaufort Sea to Baja California, Scholl, D. W., Grantz, A., and Vedder, J. G., (eds.): Houston, Texas, Circum-Pacific Council for Energy and Mineral Resources, p. 191-212.

von Huene, R., Klaeschen, D., and Fruehn, J. (1999), Relation between the Subducting Plate and Seismicity Associated with the Great 1964 Alaska Earthquake, *Pure and App. Geophys.*, 154, 575-591.

von Huene, R., J. J. Miller, and W. Weinrebe (2012), Subducting plate geology in three great earthquake ruptures of the western Alaska margin, Kodiak to Unimak, *Geosphere*, 8(3), 628–644.

Wang, K., and Hu, Y. (2006), Accretionary prisms in subduction earthquake cycles: The theory of dynamic Coulomb wedge, *J. Geophys. Res.*, 111, B06410, doi:10.1029/2005JB004094.

Wang, K. and S. Bilek (2011), Do subducting seamounts generate or stop large earthquakes? *Geology*, 39, 819-822.

Wells, R. E., R. J. Blakely, Y. Sugiyama, D. W. Scholl, and P. A. Dinterman (2003), Basin-centered asperities in great subduction zone earthquakes: A link between slip, subsidence, and subduction erosion?, *J. Geophys. Res.*, 108(B10), 2507, doi:10.1029/2002JB002072.

Young, J.B., Presgrave, B.W., Aichele, H., Wiens, D.A. and Flinn, E.A. (1996), The Flinn-Engdahl Regionalisation Scheme: the 1995 revision, *Physics of the Earth and Planetary Interiors*, 96, 223-297.

Ye, S., Flueh, E. R., Klaeschen, D., and von Huene, R. (1997), Crustal structure along the EDGE transect beneath the Kodiak shelf off Alaska derived from OBH seismic refraction data, *Geophys. J. Int.*, 130, 283-302.

Zweck, C., Freymueller, J. T., and Cohen, S. C. (2002), Three-dimensional elastic dislocation modeling of the postseismic response to the 1964 Alaska earthquake, *J. Geophys. Res.*, 107, 10.1029/2001JB000409.